© 2022. Published by The Company of Biologists Ltd | Development (2022) 149, dev200153. doi:10.1242/dev.200153

RESEARCH ARTICLE

# A prominent gene activation role for C-terminal binding protein in mediating PcG/trxG proteins through Hox gene regulation

**Cai-Li Bi[1,2,§], Qian Cheng[1,§], Ling-Yue Yan[1,*,§], Hong-Yan Wu[1], Qiang Wang[1], Ping Wang[1], Lin Cheng[1], Rui Wang[1], Lin Yang[1,‡], Jian Li[1], Feng Tie[3], Hao Xie[1,¶] and Ming Fang[1,¶]**

## ABSTRACT

The evolutionarily conserved C-terminal binding protein (CtBP) has been well characterized as a transcriptional co-repressor. Herein, we report a previously unreported function for CtBP, showing that lowering CtBP dosage genetically suppresses Polycomb group (PcG) loss-of-function phenotypes while enhancing that of trithorax group (trxG) in *Drosophila*, suggesting that the role of CtBP in gene activation is more pronounced in fly development than previously thought. In fly cells, we show that CtBP is required for the derepression of the most direct PcG target genes, which are highly enriched by homeobox transcription factors, including Hox genes. Using ChIP and co-IP assays, we demonstrate that CtBP is directly required for the molecular switch between H3K27me3 and H3K27ac in the derepressed Hox loci. In addition, CtBP physically interacts with many proteins, such as UTX, CBP, Fs(1)h and RNA Pol II, that have activation roles, potentially assisting in their recruitment to promoters and Polycomb response elements that control Hox gene expression. Therefore, we reveal a prominent activation function for CtBP that confers a major role for the epigenetic program of fly segmentation and development.

**KEY WORDS: CtBP, PcG/trxG, *Drosophila*, Transcription, Histone modification**

## INTRODUCTION

C-terminal binding proteins (CtBPs) are transcriptional co-repressors that modulate the activity of a wide-spectrum of transcription factors. Although invertebrate genomes, such as *Drosophila melanogaster*, contain a single *CtBP* gene, vertebrates possess two homologues, *Ctbp1* and *Ctbp2*, and these genes encode protein products with similar functionally conserved domain structures (Chinnadurai, 2002). Since its initial identification as a C-terminal binding partner of the viral protein E1A (Schaeper et al., 1995), the endogenous role of CtBP has been extensively studied in both invertebrate and vertebrate model systems. In *Drosophila*, CtBP plays essential roles in embryo development, acting as a co-repressor for many transcriptional repressors, such as Hairy (Poortinga et al., 1998), Krüppel, Knirps, Snail (Nibu et al., 1998a, b) and Brinker (Bi et al., 2018; Hasson et al., 2001; Yang et al., 2013). A large number of studies in mammalian cell lines have also confirmed the co-repressor role of CtBPs (Chinnadurai, 2002). CtBPs physically interact with ZEB (Postigo and Dean, 1999; Shi et al., 2003), histone deacetylases (HDACs; Subramanian and Chinnadurai, 2003) and other enzymes with histone modification activities, such as histone methyltransferases and demethylases (Shi et al., 2003), explaining the contribution of CtBP to transcriptional repression (Stankiewicz et al., 2014). Other studies have shown that human HPC2 (also known as CBX4), a chromo domain-containing protein that specifically recognizes trimethylated histone H3K27 (H3K27me3, a hallmark of repression), interacts with and sumoylates CtBP2 (Kagey et al., 2005, 2003; Sewalt et al., 1999). Although demonstration of a direct functional link is lacking in these studies, cooperation with Polycomb group (PcG) proteins might be an additional means through which CtBP exerts its repressive roles. Indeed, CtBP appears to be required for Pho (also known as YY1)-dependent recruitment of PcG proteins (Basu and Atchison, 2010; Srinivasan and Atchison, 2004), and mouse *CtBP2* is necessary for PRC2-mediated silencing in embryonic stem cells (Kim et al., 2015).

CtBPs have also been speculated to play a co-activation role in transcription, but only sporadic studies exist to support this. For example, CtBP is directly required for Wingless (Wg; a fly Wnt ligand) target expression in flies, depending on its state of homo-dimerization (Bhambhani et al., 2011; Fang et al., 2006). Recent studies have also shown that CtBPs might activate genes that promote proliferation, epithelial-to-mesenchymal transition and cancer stem cell self-renewal activity (Dcona et al., 2017) and promote NeuroD1 expression through association with the histone demethylase LSD1 (KDM1A), which removes H3K9me2 to facilitate the H3K9ac modification (Ray et al., 2014). These results indicate that CtBP may be more than just a dedicated co-repressor.

In this paper, we directly tested the role of *Drosophila* CtBP in the epigenetic regulation of gene expression. We show that reduction of *CtBP* antagonizes the leg transformation caused by mutations in PcG genes and enhances trxG-dependent phenotypes. We demonstrate using RNA-seq that CtBP is required for the derepression of more than 100 PcG target genes highly enriched by homeobox transcription factors. Furthermore, we find that CtBP interacts with many trxG proteins and potentially aids in their recruitment to Hox gene loci when derepressed. These results unveil a broader activation role for CtBP function. As CtBP interacts with both PcG and trxG proteins and functionally contributes to both transcriptional activation and repression, we propose that

[1]School of Life Science and Technology, MOE Key Laboratory of Developmental Genes and Human Diseases, Southeast University, Nanjing 210096, China. [2]Institute of Translational Medicine, Medical College, Yangzhou University, Yangzhou 225001, China. [3]Department of Genetics and Genome Sciences, Case Western Reserve University, Cleveland, OH 44106, USA.
*Present address: Department of Biomedical Engineering, University at Buffalo, The State University of New York, Buffalo, NY 14260, USA. ‡Present address: State Key Laboratory of Natural Medicines, Jiangsu Key Laboratory of Carcinogenesis and Intervention, China Pharmaceutical University, Nanjing 210009, China.
§These authors contributed equally to this work

¶Authors for correspondence (hxie@seu.edu.cn; mfang@seu.edu.cn)

H.X., 0000-0002-0683-6883; M.F., 0000-0002-7239-7604

**Handling Editor: Haruhiko Koseki**
**Received 31 August 2021; Accepted 28 April 2022**

Development (2022) 149, dev200153. doi:10.1242/dev.200153

CtBP may be important for maintaining the balance between repressive and active epigenetic players, possibly by providing a platform for a dynamic transcriptional-epigenetic switch in gene regulation.

## RESULTS

### *CtBP* genetically suppresses PcG and enhances trxG

To directly test the role of *CtBP* in the context of epigenetics, we examined the potential dose-dependent modifier function of *CtBP*, as previously reported (Kennison and Tamkun, 1988), with the rationale that the heterozygous *CtBP* phenotype in later developmental stages might be masked by its enormous maternal contribution and its essential role in the regulation of pair-rule gene expression (Nibu et al., 1998b; Poortinga et al., 1998). Heterozygous *Pc* mutant males often display extra sex combs in the second and/or third legs, commonly referred to as sex comb or leg transformations, as do mutants of other PcG genes, such as *Sex comb on midleg* (*Scm*) (Fig. 1A). In light of the several studies suggesting CtBP as a helper in PcG silencing (Basu and Atchison, 2010; Sewalt et al., 1999; Srinivasan and Atchison, 2004), we hypothesized that loss of *CtBP* would enhance the PcG sex comb transformations. Surprisingly, we found that this was not the case.

We phenotypically compared the heterozygous *Pc* ($Pc^3$/+ and $Pc^1$/+) mutant flies with flies with heteroallelic combinations of *Pc* and one of three *CtBP* alleles ($CtBP^{32P}$, $CtBP^{De10}$ or $CtBP^{Df}$) by a semi-quantitative measuring of sex comb transformations, such that they were categorized as wild type (i.e. no extra sex comb), moderate (extras only on the second legs) and strong (extras appeared on both second and third legs) transformations (Fig. 1A). Heterozygotic *CtBP* mutant flies appeared to be completely normal, fertile and with absolutely no leg transformation (Fig. 1C,D). However, we found that heteroallelic combinations of *Pc* and *CtBP* always caused less strong leg transformations than the heterozygotes of two *Pc* alleles, $Pc^3$ and $Pc^1$ (a less strong *Pc* allele); the same was observed for $Scm^{D1}$, which produced much weaker leg transformations than *Pc* (Fig. 1C). A probable more precise evaluation of the severity of leg transformation by extra sex comb teeth counting resulted in quite similar outcomes (Fig. 1D). The alleviation of the sex comb transformation of *Pc* and other PcG genes by reduction of *CtBP* indicates that *CtBP* may specifically antagonize PcG gene function.

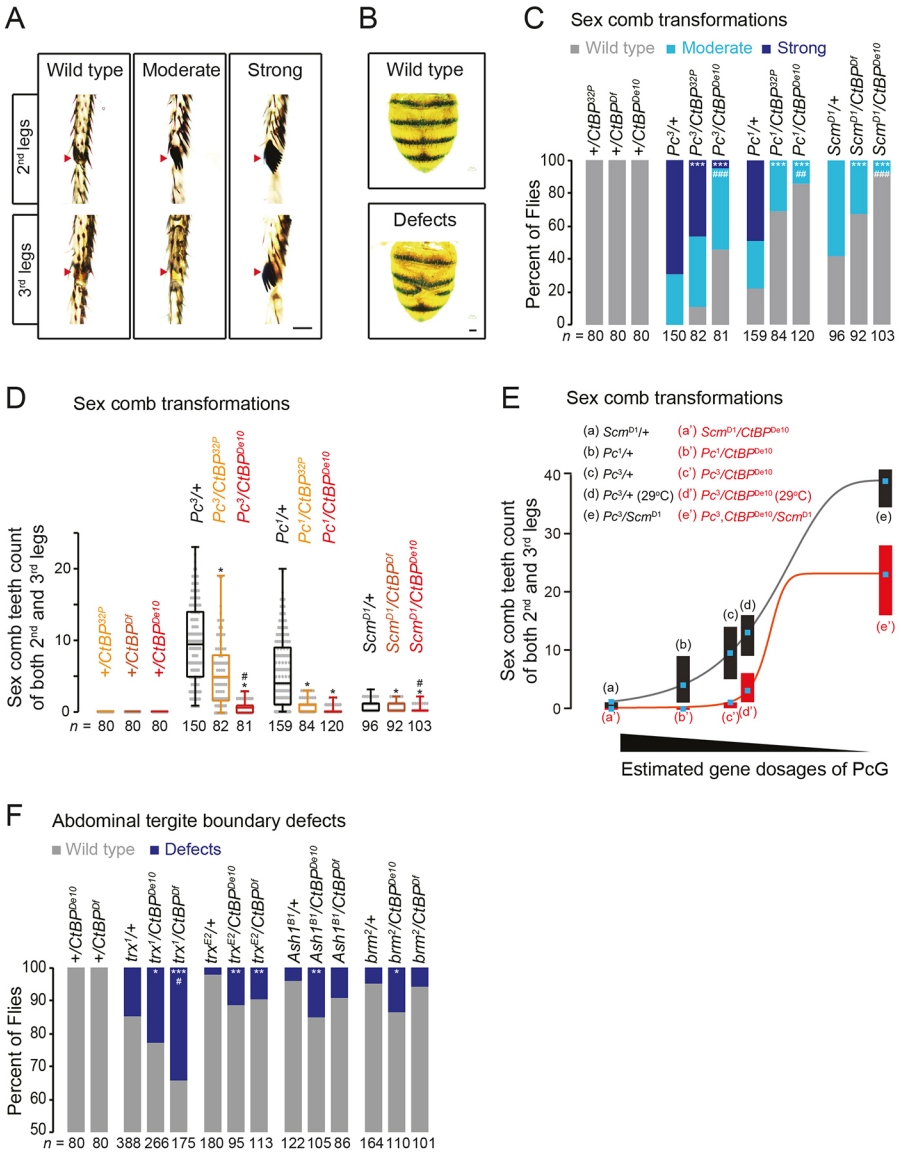


**Fig. 1. *CtBP* suppresses PcG transformations and enhances trxG phenotypes.** (A) Representative images of sex combs (arrowheads) that appeared in the second and third legs of male heterozygotic mutants of Pc ($Pc^3$/+) and the accordingly classified wild type, moderate and strong sex comb phenotypes as indicated. (B) Representative images of a wild-type abdomen and one with typical tergite boundary defect seen in heterozygotic mutants of trx ($trx^1$/+). (C) Phenotypic grading of sex comb transformations for adult males with the genotypes indicated. Strong transformations are defined by the appearance of extra sex combs in both the second and third legs, whereas moderate ones have extra sex combs only in the second legs, as in A. *n* is indicated below the stacked bars. (D) Box and whisker plots [median values (middle bars) and first to third interquartile ranges (boxes)] of total extra sex comb teeth in the second and third legs as in C. Scatter plots in gray are also shown. **P*<0.001 compared with heterozygous $Pc^1$, $Pc^3$ or $Scm^{D1}$ and $^{\#}P$<0.001 between two heteroallelic combinations (Kruskal–Wallis tests followed by Dunn's multiple comparisons tests). (E) The grading of sex comb transformations in different heterozygotic mutants, with the genotypes indicated. Note that the total extra sex comb teeth in both of the second and third legs increased with decreased PcG dosage, which was obviously abated by addition of CtBP mutation. Data are median (dots) and first to third interquartile ranges (boxes). (F) Frequencies of abdominal defects in flies with the genotypes and *n* indicated. Statistical analysis for C and E; **P*<0.05, ***P*<0.01, ****P*<0.001, compared with heterozygotic mutants of PcG or trxG genes, and $^{\#}P$<0.05, $^{\#\#}P$<0.01, $^{\#\#\#}P$<0.001 between the two heteroallelic combination groups ($\chi^2$ tests). Scale bars: 50 µm (A); 100 µm (B).

Development (2022) 149, dev200153. doi:10.1242/dev.200153

The stronger *CtBP* allele $CtBP^{De10}$ had greater alleviation effects suggests that *CtBP* may function in a gene dosage-dependent manner (Fig. 1C-E).

Given these results, we next asked whether and how *CtBP* genetically interacts with trxG genes. The prototype of trxG genes, *trithorax* (*trx*), has been extensively studied at the genetic level (Breen, 1999; Ingham, 1983), and loss of *trx* results in a variety of developmental defects including homeotic transformations of thoracic and abdominal segments (Breen, 1999; Karch et al., 1985; Singh and Mishra, 2014). Developmental defects have also been studied for other trxG genes, such as *ash1*, *ash2* and *brm* (Gindhart and Kaufman, 1995; Gutiérrez et al., 2003; Shearn, 1989). We used several previously published mutant alleles of trxG, including *trx* ($trx^1$ and $trx^{E2}$), *ash1* ($ash1^{B1}$) and *brm* ($brm^2$), to explore the genetic interaction between *CtBP* and trxG (Gindhart and Kaufman, 1995). Heterozygosity of these alleles was very rarely sufficient for a discernable haltere-to-wing transformation; however, they produced abdominal tergite boundary defects indicative for enhancement of *Pc* function (Du et al., 2016) at a considerable rate (Fig. 1B). We found that heteroallelic combinations of these mutations with *CtBP* alleles remarkably enhanced such tergite defects, even though none of them was seen in heterozygous *CtBP* mutants (Fig. 1F). Together, these data led us to the conclusion that *CtBP* genetically antagonizes PcG and enhances trxG gene functions in a gene-specific and dose-dependent manner.

### *CtBP* suppresses a *Pc* wing phenotype and is required for ectopic *Ubx* expression in *Pc* wing discs

*Pc* is known to have heterozygous wing phenotypes (Castelli-Gair and García-Bellido, 1990) and, as such, both $Pc^1$ and $Pc^3$ heterozygotes produce adult wing defects, with the strongest phenotypes displaying severe curvature, indicating a partial transformation to metathorax, and moderate ones bearing clear notches in the posterior wing edges (Fig. 2A-C). Although heterozygotic *CtBP* mutants exhibited completely normal wings, heteroallelic combination with a strong *CtBP* allele, $CtBP^{De10}$, significantly suppressed the *Pc* wing phenotypes (Fig. 2D), similar to what was observed in leg transformations (Fig. 1C,D).

As previously published (Castelli-Gair and García-Bellido, 1990; Dupont et al., 2015), $Pc^3$ is heterozygously sufficient for ectopic posterior wing pouch expression of Ultrabithorax (Ubx), presumably being derepressed by loss of *Pc* (Fig. 2E,G). As expected, heterozygotic $CtBP^{De10}$ caused no ectopic Ubx in wing discs (Fig. 2F), but it did markedly diminish the Ubx expression when heteroallelically combined with $Pc^3$ (Fig. 2G,H). Semi-quantifications of Ubx intensity indicated that those changes were significant (Fig. 2Y). We observed a similar pattern using the antibody FP6.87, which cross-recognized both Abdominal-A (Abd-A) and Ubx (Fig. 2I-L,Z), although we were unable to determine whether *abd-A*, a Hox gene member proximal to *Ubx* in the Bithorax complex (BX-C), would also be ectopically expressed in $Pc^3$ heterozygotes. The other *Ubx*-neighboring, but more distant, Hox member *Abdominal-B* (*Abd-B*) remained silent (Fig. 2M-P), whereas *Antennapedia* (*Antp*), known to have a strong wing disc expression, was not affected by the reduction of either *Pc* or *CtBP* or both (Fig. 2Q-T). Pc protein levels were slightly lower in $Pc^3$ heterozygous wing discs and were not affected by the reduction of *CtBP* (Fig. 2U-X), which we confirmed using RT-qPCR (Fig. S1A). To provide a possible explanation of the notch phenotypes seen in adult wings (Fig. 2B), we stained wing discs for Distal-less (Dll), a Wg target important for wing development. We found an obvious correlation between the ectopic Ubx expression and the reduction of Dll in the posterior wing pouch (Fig. S2). We therefore demonstrated that *CtBP* is required for the derepression of *Ubx* (and possibly *abd-A*) caused by loss of *Pc*, which in turn negatively influences the Wg signaling pathway and results in the defective wings. These data indicate that *CtBP* may antagonize *Pc* function at the level of gene expression.

### *CtBP* is required for the transactivation of many PcG-repressed transcription factors

To further explore the role of *CtBP* on PcG target genes and to extend our genetic findings to a genome-wide level, we used a cell model of PcG target derepression as previously reported (Fang et al., 2009; Schwartz et al., 2006). Briefly, we used combinational RNAi for PcG and *CtBP* in *Drosophila* Kc167 (Kc) cells and observed the differential expression of PcG target genes using RNA-seq. As expected, double RNAi of *polyhomeotic proximal* (*ph-p*) and *Enhancer of zeste* [*E(z)*], both of which encode core components of polycomb repressive complexes (PRCs), caused expression and/or derepression of many genes, or PcG repressed genes, of which we selected 381 genes for further analyses based on their expression changes being significantly increased by more than twofold (Fig. S3). Co-knockdown of *CtBP* with *ph-p* and *E(z)* caused different effects on gene expression and clustered these PcG repressed genes into three categories (Fig. 3A; Table S2; see also Materials and Methods for detail). Strikingly, we found that *CtBP* is required for the expression of 153 (~40%) of the PcG repressed genes and we grouped them as *CtBP* co-activated genes (Fig. 3A). For genes for which expression levels are not significantly affected (143, ~38%) or enhanced (85, ~22%) by co-depletion of *CtBP*, we created *CtBP* unaffected genes and *CtBP* co-repressed genes, respectively (Fig. 3A). We next examined these three groups of genes using DAVID Functional Category analysis (Huang et al., 2009) and found that the *CtBP* co-activated gene group was highly enriched with transcription factors and developmental proteins and, most prominently, the homeobox transcription factors (Fig. 3B). The group of genes not regulated by *CtBP* was enriched by transcription factors as well but with much less confidence (Fig. 3B). In sharp contrast, *CtBP* co-repressed genes were bereft of any significant functional enrichment. Consistent with the DAVID analysis, Gene Ontology (GO) detailed *CtBP* co-activated genes with respect to both molecular function and biological process, and highlighted the gene function enrichment of transcription and development (Fig. 3C,D). These results suggest that the prominent function of CtBP in the context of PcG relief may be gene activation.

An important question to answer is whether CtBP might act the same fashion for direct PcG targets. It is almost certain that PcG may not repress all of the 381 genes directly and it will be a difficult task to define or identify the bona fide Pc targets by simple rules. However, we suggest that the combination of the genome-wide profile of Pc and the derepression could be a good indicator. Therefore, we assumed that the intersection of 73 genes from the 381 used in Fig. 3 and the 333 with strong PcG binding sites (Schwartz et al., 2006) were most likely to be direct PcG targets (Fig. 4A; Table S3). Interestingly, cluster analysis categorized most of these PcG targets (65, ~89%) as *CtBP*-associated PcG targets, whereas only a handful of them (8, ~11%) were *CtBP*-unassociated PcG targets (Fig. 4B; Table S3). Importantly, DAVID Functional Category analysis generated a similar functional enrichment chart of the 65 *CtBP*-associated PcG targets with even higher confidences of

Development (2022) 149, dev200153. doi:10.1242/dev.200153

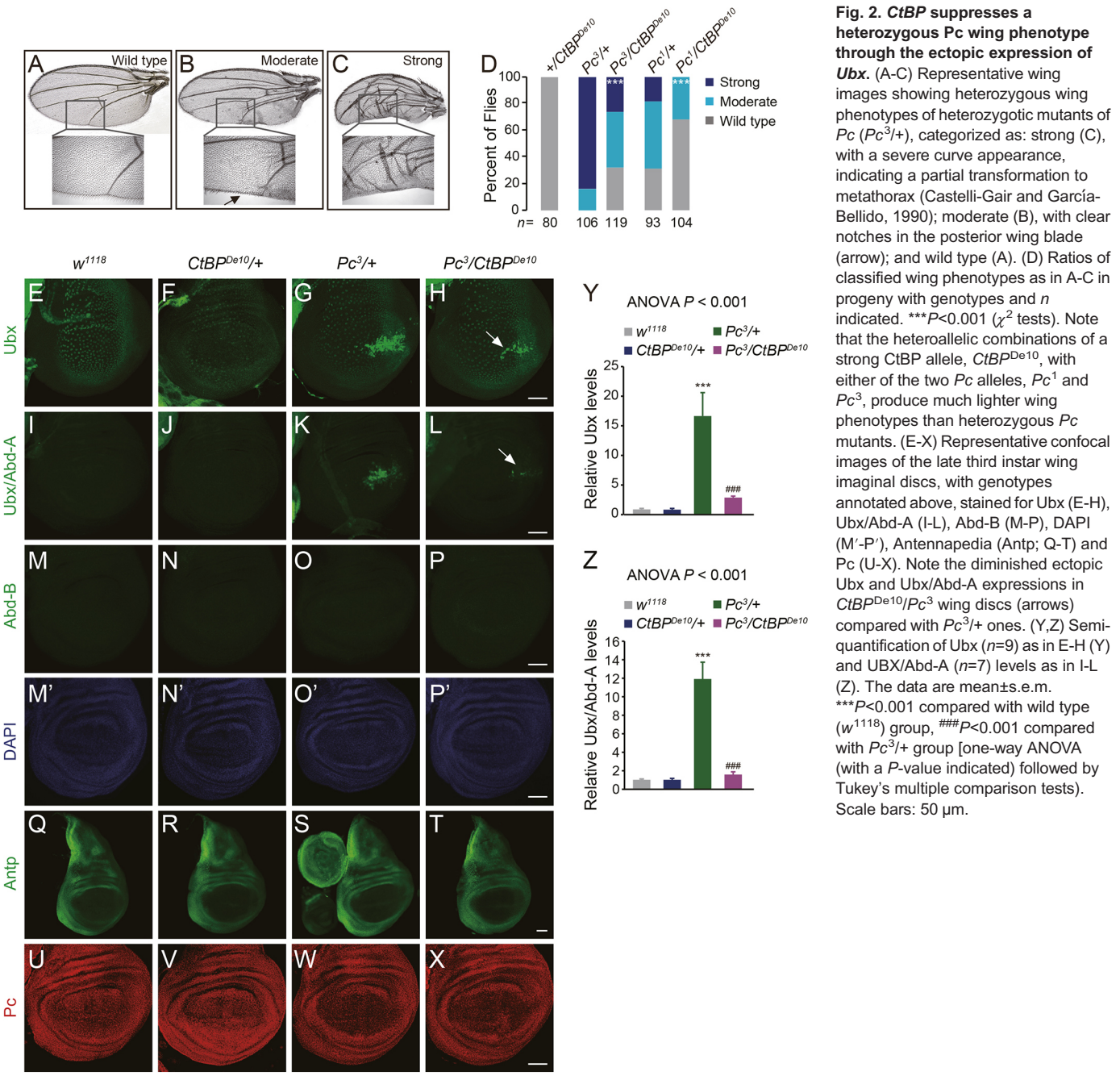


**Fig. 2. *CtBP* suppresses a heterozygous Pc wing phenotype through the ectopic expression of *Ubx*.** (A-C) Representative wing images showing heterozygous wing phenotypes of heterozygotic mutants of *Pc* ($Pc^3$/+), categorized as: strong (C), with a severe curve appearance, indicating a partial transformation to metathorax (Castelli-Gair and García-Bellido, 1990); moderate (B), with clear notches in the posterior wing blade (arrow); and wild type (A). (D) Ratios of classified wing phenotypes as in A-C in progeny with genotypes and *n* indicated. ***$P$<0.001 ($\chi^2$ tests). Note that the heteroallelic combinations of a strong CtBP allele, $CtBP^{De10}$, with either of the two *Pc* alleles, $Pc^1$ and $Pc^3$, produce much lighter wing phenotypes than heterozygous *Pc* mutants. (E-X) Representative confocal images of the late third instar wing imaginal discs, with genotypes annotated above, stained for Ubx (E-H), Ubx/Abd-A (I-L), Abd-B (M-P), DAPI (M′-P′), Antennapedia (Antp; Q-T) and Pc (U-X). Note the diminished ectopic Ubx and Ubx/Abd-A expressions in $CtBP^{De10}/Pc^3$ wing discs (arrows) compared with $Pc^3$/+ ones. (Y,Z) Semi-quantification of Ubx ($n$=9) as in E-H (Y) and UBX/Abd-A ($n$=7) levels as in I-L (Z). The data are mean±s.e.m. ***$P$<0.001 compared with wild type ($w^{1118}$) group, ###$P$<0.001 compared with $Pc^3$/+ group [one-way ANOVA (with a $P$-value indicated) followed by Tukey's multiple comparison tests). Scale bars: 50 µm.

homeobox genes (Fig. 4C), and about two thirds (49, ~67%) of the 73 PcG targets were DNA-binding proteins (Fig. 4C). Therefore, it is most likely that *CtBP* is highly and selectively required for the activation of PcG targets, in particular, the homeobox transcription factors, including Hox genes. The fact that *CtBP* knockdown affects the derepression of PcG genes in both directions suggested that the CtBP effects are unlikely to be caused by the fluctuations of RNAi efficiency. Nevertheless, we have confirmed the knockdown levels for every gene subjected to RNAi in each experiment by RT-qPCR and/or western blots (Fig. S1B-F). In addition, we used RT-qPCR to verify the effect of CtBP on the derepression of four Hox genes, *Antp*, *Ubx*, *abd-A* and *Abd-B* (Fig. 4D-G). Importantly, knockdown of *Pc* alone was sufficient to derepress these Hox genes, and we observed similar subdued derepression effects with the addition of *CtBP* RNAi (Fig. 4H-K). At the same time, knockdown of *CtBP* alone exerted minimal effects on expression of these genes (Fig. 4D-K). These results indicate that *CtBP* plays a modulatory activation role in the dynamic regulatory processes of PcG target genes, such as derepression, not through modulating any specific PRC component. We thus unveil a previously unsuspected prominent transcriptional activation function for *CtBP* in the context of epigenetics.

### CtBP is directly required for the molecular switch from H3K27me3 to H3K27ac histone modifications, possibly through the recruitment of CBP and UTX to the derepressed Hox loci

To examine whether CtBP activates PcG target genes directly or indirectly, we performed chromatin immunoprecipitation (ChIP)-qPCR assays at several Hox gene regulatory sites (Beisel et al.,

Development (2022) 149, dev200153. doi:10.1242/dev.200153

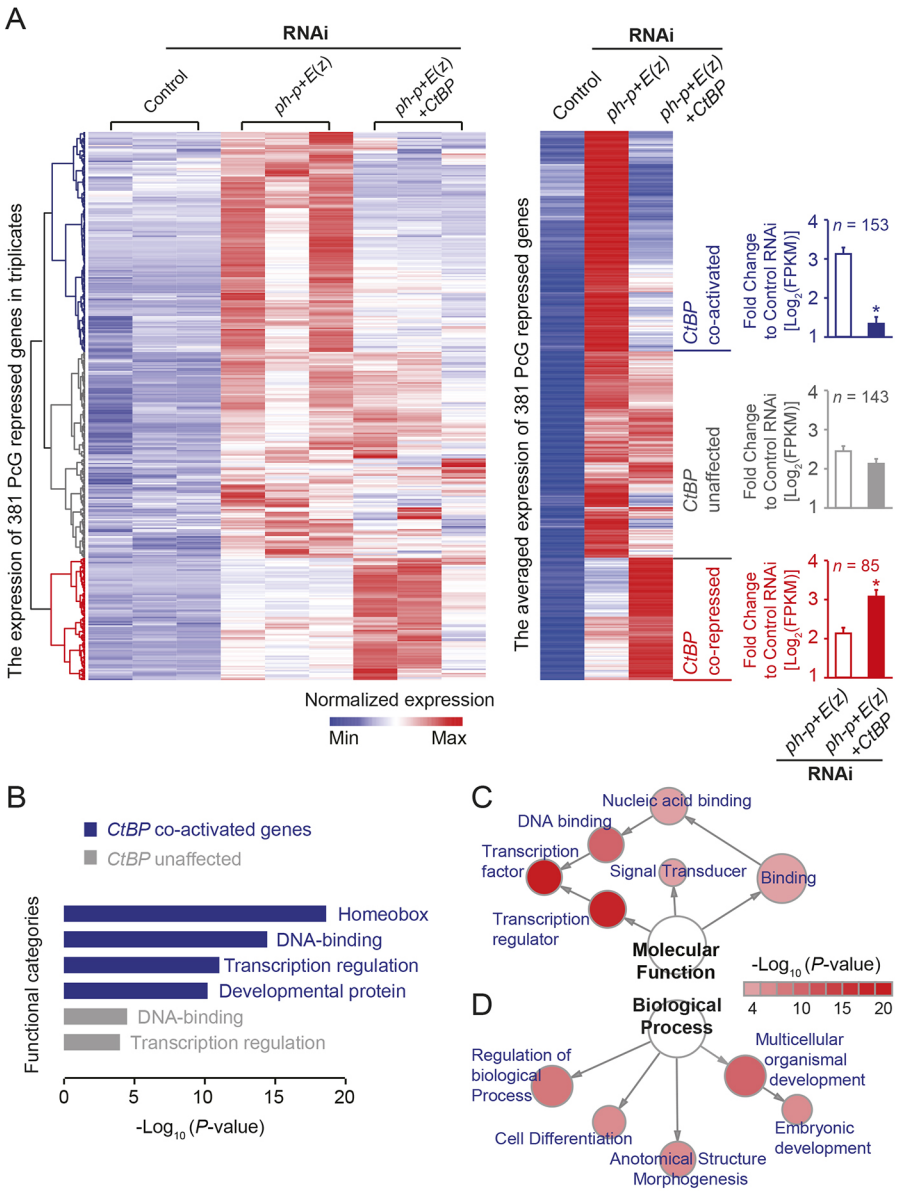


**Fig. 3. *CtBP* is required for the expression of a functionally selective subset of PcG repressed genes in Kc cells.** (A) Heat maps of normalized expression values (FPKM) listed in order of supervised hierarchical clustering (Ward's method) of RNA-seq data for 381 PcG repressed genes (see Fig. S3) in different RNAi-treated Kc cells as indicated, in triplicates and averages as indicated. Also, shown to the right are the averaged $Log_2$ fold changes (mean±s.e.m.) of the three major clusters, grouped as *CtBP* co-activated (blue), *CtBP* unaffected (gray) and *CtBP* co-repressed (red). **P*<0.001 (one-way ANOVA followed by Newman-Keuls multiple comparisons tests). (B) Functional categories analysis of *CtBP* differentially regulated PcG repressed genes as grouped in A by DAVID (see Materials and Methods for detail). $\alpha$=0.01. Note that homeobox genes were enriched with the highest confidence coefficient in the *CtBP* co-activated gene group, whereas no significant gene enrichment was found in the *CtBP* co-repressed one. (C,D) GO charts of Molecular Functions (C) and Biological Processes (D) for PcG repressed genes of the *CtBP* co-activated gene group, analyzed and visualized as directed acyclic graphs with Cytoscape (see Materials and Methods for details). GO categories are shown in circles with the area proportional to the ratios of observed gene frequencies over expected ones; the intensity of the red correlates with minus $Log_{10}$ (*P*-values) as indicated by the gradient bar. Note that the transcription factors/regulators are highlighted by GO Molecular Functions (C) and the prominent cell differentiation and development functions are highlighted in GO Biological Processes (D).

2007; Müller and Bienz, 1991; Orlando et al., 1998; Papp and Müller, 2006; Schwartz et al., 2006; Simon et al., 1993; Zink and Paro, 1995), including Polycomb response elements (PREs) and/or proximal promoter regions (promoter) in both the Antennapedia gene complex (ANT-C) and BX-C, and an intergenic site for the negative binding of Pc (Fig. 5A). *CtBP* RNAi alone caused dramatic decreases in CtBP ChIP signals at *Antp and Ubx* sites, indicating physically direct occupation of CtBP (Fig. 5B; Table S4-1), and it is worth noting that PcG RNAi caused little change of CtBP binding at the three PREs but lowered binding at the proximal promoter sites (Fig. 5B; Table S4-1). These results suggest that CtBP might preferentially stay at the PREs rather than the proximal promoters upon the relief of PcG repression. Knockdown of *CtBP* alone resulted in a reduced, but not significantly, Pc occupation along with the related H3K27me3 histone mark (Fig. 5C,D; Tables S4-2,S4-3), which could be consistent with the published studies (Basu and Atchison, 2010; Srinivasan and Atchison, 2004).

For PcG RNAi cells, the impact of CtBP was more dramatic. As expected, PcG RNAi resulted in significantly lower Pc binding and H3K27me3 levels, with higher levels of CBP and UTX bindings and H3K27ac modifications (Fig. 5), consistent with the derepression of *Ubx* and *Antp* (Fig. 4D-K). However, when PcG RNAi was combined with *CtBP* knockdown, these repression and activation marks were abolished (Fig. 5C-G; Table S4), indicating that reduction of *CtBP* completely prevented the repression/activation mark switch and provides a molecular explanation that CtBP is required for the derepression of PcG targets, such as *Ubx* and *Antp*. We were intrigued with two seemingly puzzling observations that when both *E(z)* and *ph-p*, which encode the catalytic subunit for H3K27me3 and a Pc-interacting key component of PRC1, respectively, were knocked down, co-knockdown of *CtBP* maintained high levels of Pc binding and H3K27me3 levels (Fig. 5C,D; Tables S4-2 and S4-3). One possible explanation could be that CtBP helped the recruitment of UTX, the major H3K27me3 demethylase, to the derepressed Hox sites. Therefore, loss of *CtBP* might cause the stabilization of the H3K27me3 mark, which in tune recruits Pc through the Chromo domain. In other words, CtBP might facilitate the removal of the repressive proteins or histone marks upon the derepression of the Hox genes. This might be mechanistically different from the result

Development (2022) 149, dev200153. doi:10.1242/dev.200153

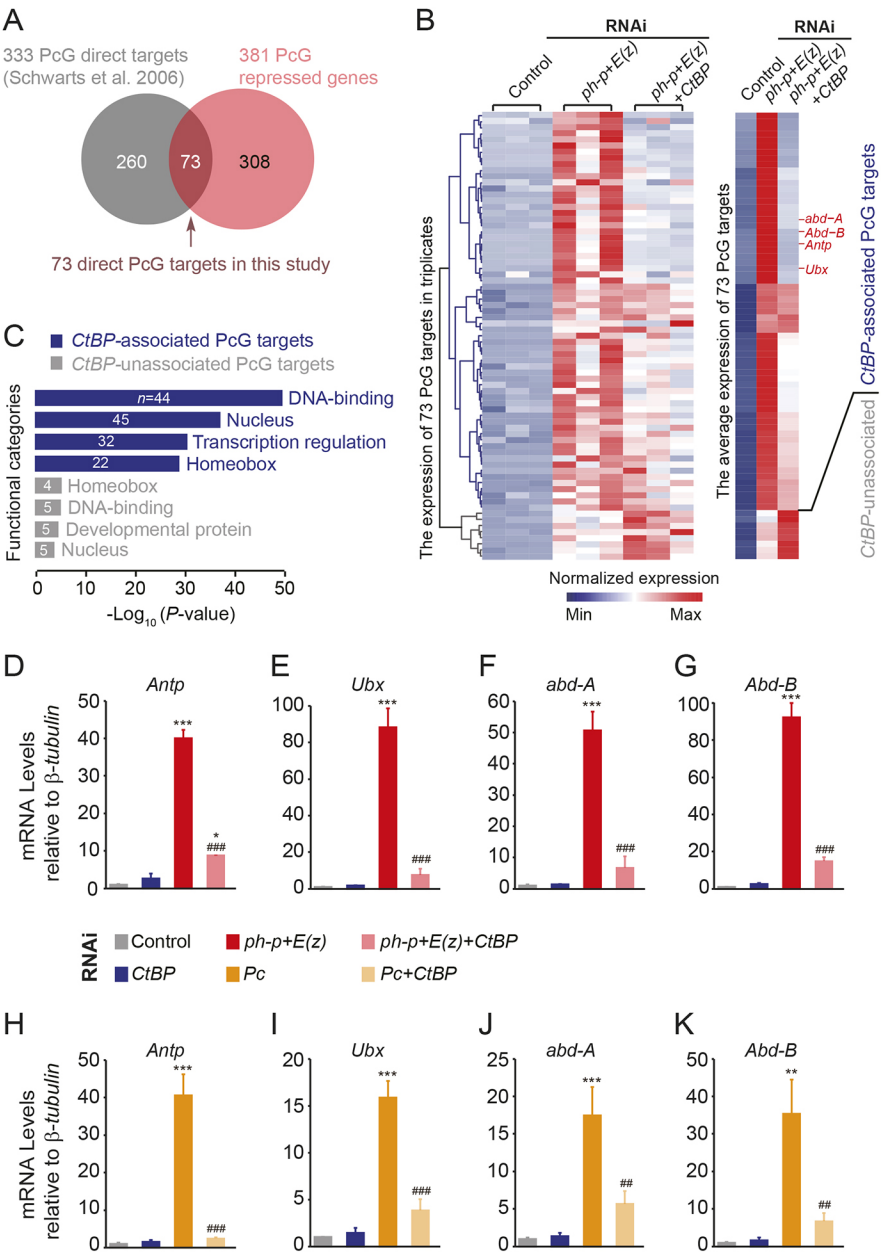


**Fig. 4. *CtBP* is required for the expression of the most PcG targets.** (A) Venn diagram showing the 381 PcG repressed genes in Fig. 3A and the 333 potential PcG direct targets previously published (see Materials and Methods for detail). The intersection (arrow) represents 73 direct PcG targets that were derepressed upon the depletion of both *E(z)* and *ph-p* in Kc cells, which we used for further analyses. (B) Heat maps of the normalized expression of the 73 PcG targets (A) as in Fig. 3A, categorized as *CtBP*-associated and -unassociated PcG targets. The four genes marked in red were verified further by RT-qPCR in D-K. (C) Functional categories analysis of the 65 CtBP-associated PcG targets in B by DAVID (Fig. 3B; see Materials and Methods for details), with the α value set to 0.01. (D-K) Representative qRT-PCR quantifications of the expression of four indicated Hox genes in Kc cells with different combinations of RNAi treatments. Experiments were performed in triplicate and repeated at least three times. The data are expressed as mean±s.e.m. **P*<0.05, ***P*<0.01, ****P*<0.001 compared with control group, $^{\#\#}P$<0.01, $^{\#\#\#}P$<0.001 compared with *ph-p+E(z)* RNAi or *Pc* RNAi group (one-way ANOVA, followed by Tukey's multiple comparison tests). Note that *Pc* RNAi alone was sufficient for the derepression of all Hox genes tested.

that loss of CtBP caused moderate reductions of Pc and a subtle decrease of H3K27me3 level without significant difference, when the Hox genes were barely expressed and the UTX levels were kept low (Fig. 5C,D; Tables S4-2 and S4-3).

To further explore this matter, we carried out co-immunoprecipitation (co-IP) experiments to show that CtBP indeed physically interacted with both UTX and CBP (Fig. 5H; Fig. S4). Reciprocal co-IPs confirmed these protein-protein interactions (Fig. 5I,J; Fig. S4). We also used ethidium bromide (EB) treatment to eliminate the probable DNA mediated interactions (Fig. 5H-J). These results indicate that CtBP interacts with many proteins to affect gene activation and support a model that CtBP is required for UTX and CBP chromatin recruitment to promote the molecular switch between H3K27me3 and H3K27ac.

Taken together, these data indicate that CtBP might play a role in the orchestration of epigenetic regulators and histone modifications in the course of dynamic switching between repression and activation of Hox genes.

## CtBP is required for RNA Polymerase II promoter bindings and phosphorylation at Ser2 through binding at the PREs

We next asked whether CtBP had direct impact on the transcription initiation and elongation in the context of Hox gene regulation by PcG/trxG. For this purpose, we tested the chromatin bindings of RNA Polymerase II [with αC-terminal domain (CTD)], as well as its phosphorylated forms at Ser2 (αSer2-P), which are required for gene initiation and elongation, respectively (Komarnitsky et al., 2000; Samkurashvili and Luse, 1998). The ChIP results by αCTD and αSer2-P showed different influences of the reduction of PcG and *CtBP* functions. PcG knockdown caused remarkable increase of αCTD signals in the proximal promoter regions (Fig. 6A; Table S4-7) and αSer2-P signals in both PREs and promoters of Antp and bxd (Fig. 6B; Table S4-8), indicating that the relief of PcG repression automatically promoted the initiation and elongation of transcription and were consistent with the prominent derepression of the PcG targets (Figs 3 and 4). Apparently, co-knockdown of *CtBP* diminished such increases, suggesting a requirement of *CtBP* in

Development (2022) 149, dev200153. doi:10.1242/dev.200153

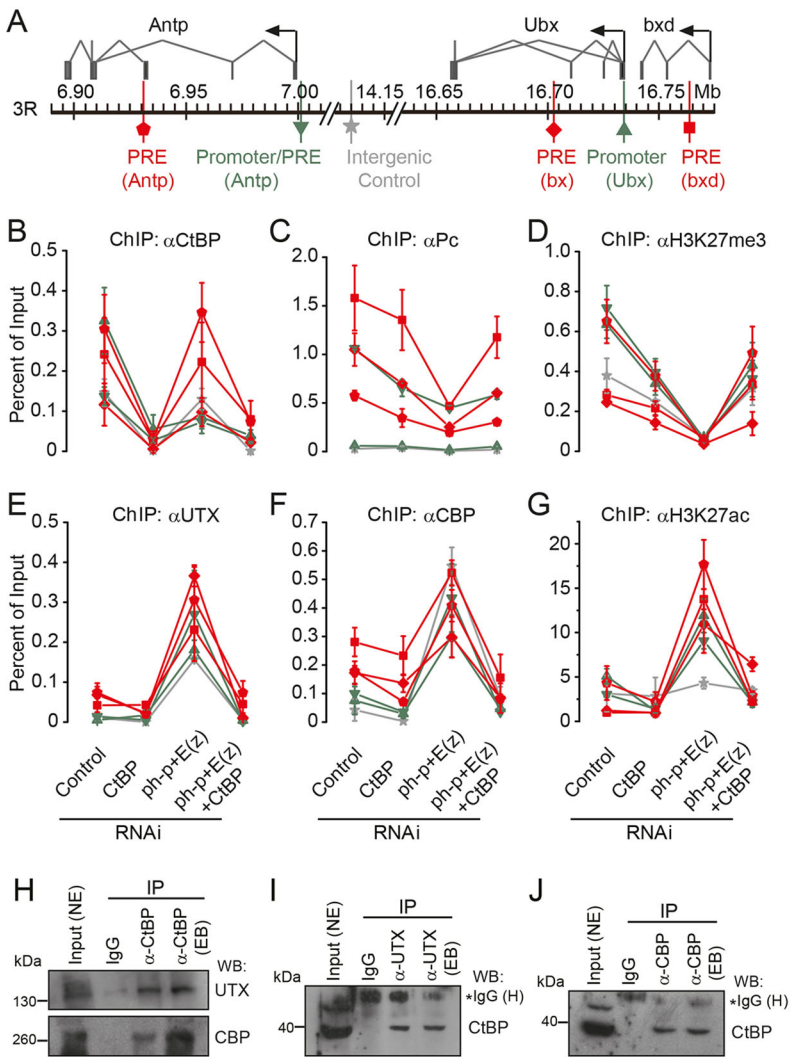


**Fig. 5. CtBP is required for the histone modification switch and the recruitments of CBP and UTX, upon depletion of PcG genes, in the derepressed Hox loci.** (A) Schematic showing the select regulatory sites, including PREs (red), promoter (green) and promoter/PRE (green) in ANT-C and BX-C complexes as indicated by polygons and gene names (in brackets) for ChIP-qPCR assays. Also shown is an intergenic control site (gray pentacle). (B-G) ChIP-qPCR signals were measured using antibodies as indicated in Kc cells with different RNAi treatments. The data are from triplicate measurements and expressed as the mean±s.e.m. Note that *CtBP* RNAi caused reversal of the changes of H3K27ac/H3K27me3 histone marks and the bindings of UTX, CBP and Pc in the context of loss of PcG genes [i.e. *ph-p* and *E(z)*]. The statistical analysis for ChIP-qPCR was performed using one-way ANOVA followed by Tukey's multiple comparison tests (Table S4). (H-J) Western blots by antibodies indicated (to the right) of nuclear extracts (NE, 10% input), co-immunoprecipitates (IP) of normal IgG (IgG) and the indicated antibodies in Kc cells. Co-IP was performed in the presence or absence of ethidium bromide (EB) to eliminate the DNA-mediated protein associations.

both transcription initiation and elongation (Fig. 6A,B; Table S4). Furthermore, the massive elevations of αSer2-P signals in PREs in derepressed Hox loci emphasized the significant regulatory role of PREs, and were consistent with our results that CtBP might preferentially operate on PREs (Figs 5B and 6A; Table S4).

Indeed, we found physical interactions between CtBP and the phosphorylated form of RNA polymerase II (Ser2-P) (Fig. 6C). In addition, CtBP interacted with Fs(1)h (Fig. 6C), the fly homologue of BRD4, a candidate kinase of RNA Pol II (Steffen and Ringrose, 2014). By confirming the interactions between RNA Pol II Ser2-P, Fs(1)h, CBP and UTX (Fig. 6D-F, Fig. S4), our results suggested that CtBP may be directly required to achieve active transcription of Hox genes by interacting with epigenetic coactivators (i.e. CBP and UTX) and the core transcriptional machinery including RNA Pol II Ser2-P and Fs(1)h.

## DISCUSSION

For over two decades, CtBP has been extensively studied in both invertebrate and mammalian model systems. CtBP physically interacts with a large number of sequence-specific DNA binding proteins and mediates their transcriptional activities. Although the prevailing model is that CtBP functions as a co-repressor for these DNA binding factors, its major biological function *in vivo* remains controversial, particularly during the course of animal development. In *Drosophila*, genetic studies have shown that *CtBP* may both enhance and repress gene expression in a transcription factor-dependent manner (Nibu et al., 1998b; Phippen et al., 2000; Poortinga et al., 1998). In mice, the co-repressor role of CtBP does not sufficiently explain the deficits found in both *CtBP1* and *CtBP2* mutant mice. Rather, the study suggests that CtBPs may contribute equally to gene repression and activation (Hildebrand and Soriano, 2002). Thus, the question remains: which one is more important for the *in vivo* function of CtBP, repression or activation?

Answering this question is not an easy task owing to the apparent pleiotropic nature of CtBP. In *Drosophila*, loss of *CtBP* severely disrupts the embryonic body plan and inhibits early embryonic regulators, including many of the pair-rule genes and potentially some gap genes (Nibu et al., 1998a; Poortinga et al., 1998), preventing further investigation on its role in later developmental stages. In particular, it is quite difficult to dissociate the direct action of CtBP on Hox from its role on pair-rule genes, which in turn affect Hox expression. This scenario might help to explain in part why genetic studies in mouse are not particularly informative (Hildebrand and Soriano, 2002).

To circumvent this difficulty, we examined the role of CtBP in the epigenetic context. We found that *CtBP* suppresses PcG homeotic transformations and enhances those of trxG (Fig. 1). Therefore, *CtBP* may function as a dose-dependent modifier of the major epigenetic regulators, opposing its co-repressor role in fly development. *Pc* transformations have at least partially known

Development (2022) 149, dev200153. doi:10.1242/dev.200153

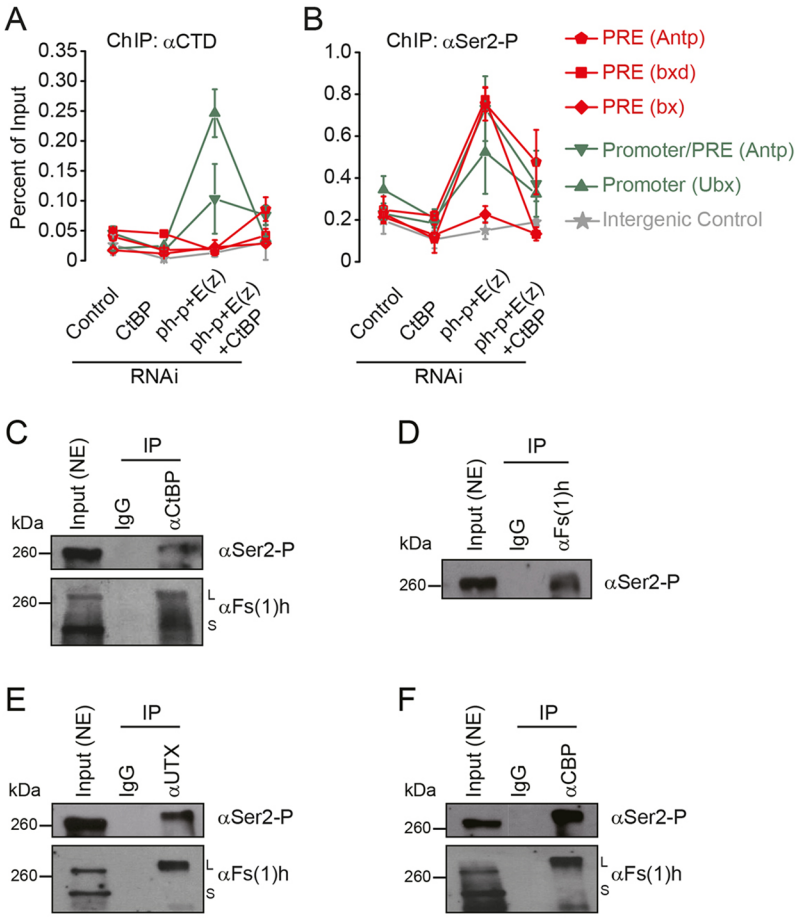


**Fig. 6. CtBP is required for loss of PcG-caused binding and phosphorylation of RNA Polymerase II in the promoter/PRE regions in Hox loci.** (A,B) ChIP-qPCR signals were measured using the antibodies indicated and expressed as in Fig. 5. Note that *CtBP* depletion caused reversal of the occupations of both RNA Polymerase II Ser2-P (Ser2-P) and RNA Polymerase II (CTD) in the promoter regions. The statistical analysis for ChIP-qPCR in Figs 5 and 6 was performed by using one-way ANOVA followed by Tukey's multiple comparison tests (Table S4). (C-F) Western blots using antibodies indicated, including one specific for RNA Polymerase II Ser2-P (αSer2-P), in nuclear extracts (NEs) and co-immunoprecipitates (IP) by normal IgG (IgG) and antibodies indicated (on top) in Kc cells. Co-IP was carried out in the presence of ethidium bromide to eliminate DNA-mediated protein associations. For reasons we do not understand, Fs(1)h bands resulting from co-IP were always with a lag compared with input in the blots. L, long form of Fs(1)h; S, short form of Fs(1)h.

gene bases, such as those we demonstrated with ectopic expression of *Ubx* in the wing discs (Fig. 2) and *Sex combs reduced* in leg discs shown by other studies (Pattatucci and Kaufman, 1991). Therefore, the fact that CtBP suppresses *Pc* transformations may suggest or reflect an altered embryonic Hox pattern that was too delicate to be observed. Importantly, the heteroallelic combination strategy that we employed in this study allowed us to dissociate the role of CtBP in earlier embryonic development from later stages and led to the finding that activation may be a prominent function for CtBP during the course of development. Although it is hard to tell whether CtBP acts directly to modulate PcG and trxG functions in these *in vivo* experiments, it is most likely that *CtBP* may function in a parallel temporal fashion with *Pc*, as neither altered expression of pair-rule genes, such as *even skipped* and *fushi tarazu*, nor any defect in adult flies was discernable for heterozygous *CtBP* alleles.

In agreement with our *in vivo* studies, we have demonstrated, using RNA-seq analyses in embryonic-derived Kc cells, that *CtBP* plays an essential activation role in the regulation of most direct PcG targets, having the highest enrichment of homeobox transcription factors (Figs 3 and 4). In sharp contrast, *CtBP*, in conjunction with PcG, co-represses a relatively smaller proportion of genes with diverse functions, among which only a handful may potentially direct PcG targets. These findings might suggest that *CtBP* has a prominent activation role that is highly selective for developmental transcription factors, including Hox genes, whereas the repressive role of *CtBP* is unspecific and possibly irrelevant with PcG repression. Using ChIP and co-IP assays, we further provide evidence that CtBP physically interacts with CBP and UTX, helping to recruit these histone modifiers to several well-characterized regulatory sites in Hox loci. Accordingly, CtBP is required to coordinate the switch from a repressive H3K27me3 form to an active H3K27ac mark (Fig. 5). For the sake of inspiration, we would imagine a wider function of CtBP in rewiring epigenetic networks composed by various kinds of histone modifications and other marks. For example, it has been proposed that H3K27ac signal coincides with H3K4me3, which constitutes a key part of the molecular mechanism of antagonizing Pc silencing (Tie et al., 2009). Indeed, our results might allow us to favor a model in which CtBP constitutes part of a large complex including many epigenetic writers and erasers, such as CBP and UTX, closely working with the core transcriptional machinery centered by RNA Pol II (Figs 5 and 6). Therefore, CtBP may play a profound role in PcG/trxG-mediated Hox gene regulation.

Although many biochemical studies have indicated that CtBPs are mainly associated with repressive histone modifiers (Shi et al., 2003), it is noteworthy that these studies were mostly performed in cell lines with a static gene expression status and so may not properly reflect the dynamic changes of transcriptional programs *in vivo*. Furthermore, the previously identified CtBP-interacting proteins are not dedicated transcriptional repressors/co-repressors. As such, there are examples illustrating the requirement of LSD1 and some of the HDACs for transactivation (Ray et al., 2014; Wirén et al., 2005). However, CtBP has been reported by others to interact with proteins for gene activation. For example, it has been documented in detail that CtBP1 directly binds to the bromodomain of p300 (Kim et al., 2005), coincident with our findings that CtBP interacts with CBP in flies (Fig. 5H,J).

Development (2022) 149, dev200153. doi:10.1242/dev.200153

Together, our findings highlight a direct and prominent activation role of CtBP in early fly development stages, probably no later than the determination of segment identities when *Pc* and Hox genes are acting. Mechanistically, CtBP could play its coactivator role in the dynamic switch or establishment of proper chromatin structures for prolonged gene activation by recruiting histone modifiers such as CBP and UTX. Alternatively, CtBP might play roles in both activation and repression, functioning in the balance between PcG and trxG actions (Piunti and Shilatifard, 2016). For example, it could be that CtBP activates in PREs or enhancers but represses at promoters, as shown by the unchanged CtBP occupation upon PcG depletion (Fig. 5B). Significantly, unlike previous findings that CtBP only activates genes in exceptional cases, we have provided evidence that CtBP directly activates gene expression in the major developmental processes, such as the precise patterning of Hox genes, indicating that activation is probably an important role for CtBP in the context of development. We have thus uncovered a gene co-activation role for CtBP *in vivo* that might have been previously masked due to its impact on the earlier developmental regulators.

It will be intriguing to know whether CtBP activates PcG targets beyond Hox genes or an opposite mechanism exists, as in mouse ESC differentiation, in which CtBP2 couples with NuRD-mediated deacetylation (18) for our identified CtBP-unassociated PcG targets. In mouse, the loss of CtBP2 causes incomplete ESC differentiation, a process known to be dependent upon gene activation (Betschinger et al., 2013; Tarleton and Lemischka, 2010). Our finding could provide an alternative interpretation, if the prominent gene activation role of CtBP were conserved in mouse. Given the complexity of the role of CtBP in cancers (Ding et al., 2020; Wu et al., 2021), our findings might provide additional data that can be used towards the development of novel strategies based on CtBP as a therapeutic target.

## MATERIALS AND METHODS

### *Drosophila* genetics

All fly lines were cultured on standard medium at 25°C. Three *CtBP* alleles were used in this study: the strong $CtBP^{87De-10}$ allele and the less strong $CtBP^{03463}$ allele (also known as $CtBP^{P1590}$), which we referred to as $CtBP^{De10}$ and $CtBP^{32P}$, have been previously described (Poortinga et al., 1998), and a *CtBP* deficiency [*Df (3R) Exel8157*] line ($CtBP^{Df}$) from the Exelixis collection (Parks et al., 2004), which has nearly the entire coding region of CtBP removed. PcG/trxG alleles, including $Pc^1$, $Pc^3$, $Scm^{D1}$, $trx^1$, $trx^{E2}$, $brm^2$ and $ash1^{B1}$, have been previously described (Duncan, 1982; Gindhart and Kaufman, 1995; Kennison and Tamkun, 1988; Lewis, 1978): $Pc^3$ is an extreme antimorphic allele, whereas $Pc^1$ is a less extreme amorphic allele of *Pc*. All stocks were from the Bloomington Drosophila Stock Center and we used $w^{1118}$ as the wild-type control allele. All the crosses were carried out at 25°C.

To test the genetic interactions between *CtBP* and the PcG/trxG genes, male *CtBP* alleles over TM6B balancer or $w^{1118}$ were crossed to virgin PcG/trxG alleles also over a TM6B balancer to generate heterozygotes of PcG/trxG mutants or heteroalleotic combinations of CtBP alleles over PcG/trxG ones. For semi-quantitative assay of sex comb transformations, adult male progenies were assessed for extra sex combs in the second and third legs. Posterior wing phenotypes and abdominal segment defects were scored as previously described (Castelli-Gair and García-Bellido, 1990; Du et al., 2016). For wing phenotype observation, adult wings were dissected in isopropanol and mounted to onto glass slides with Euparal mounting media (BioQuip). All images were acquired using a MZ16F stereomicroscope equipped with a QImaging digital camera (Leica).

### Antibodies

Rabbit polyclonal antibodies against CtBP (Fang et al., 2006), UTX (Zhang et al., 2013), Pc, CBP and Fs(1)h (Tie et al., 2016) have been previously described. Mouse monoclonal anti-Ubx (FP3.38) was kindly supplied by Dr White (White and Wilcox, 1984). Mouse monoclonal anti-Ubx/Abd-A (FP6.87), anti-Abd-B (1A2E9) and anti-Antp (8C11) were obtained from the Developmental Studies Hybridoma Bank. Rabbit polyclonal anti-Dll was kindly provided by Sean Carroll (Panganiban et al., 1995). Rabbit anti-H3K27ac (ab4729), mouse anti-H3K27me3 (ab6002), mouse anti-RNA Pol II (8WG16, ab817) and rabbit anti-RNA Pol II Ser2-P (ab5095) were from Abcam. Note that the monoclonal antibody 8WG16 (αCTD) primarily recognizes the non-phosphorylated CTD repeat within the Rpb1 subunit, which may be used as an indication of the initiation of gene transcription. The rabbit anti-RNA Pol II Ser2-P (αSer2-P, ab5095, Abcam) specifically recognizes the Ser2 phosphorylation and reflects the elongation process of transcription. Rabbit anti-IgG, mouse anti-IgG and mouse anti-tubulin were purchased from Sigma-Aldrich.

Immunostaining of wing imaginal discs were carried out as previously described (Fang et al., 2006) with anti-Ubx (1:20), anti-Ubx/Abd-A (1:100), anti-Abd-B (1:100), anti-Antp (1:20), anti-Pc (1:200) and anti-Dll (1:100). All images were collected using an Axiophot (Zeiss) coupled to a Carl Zeiss LSM 710 confocal apparatus (Zeiss). For semi-quantification of immunostaining in the wing discs, single color channels were processed into inversed and grayscale mode in Photoshop (Adobe, v11.0) and the mean gray values were measured for area with signal and subtracted by one without signal (in the anterior compartment) using ImageJ (National Institutes of Health, v1.46), and served as index for quantification.

### *Drosophila* cell culture experiments

Kc cells were cultured and RNAi treated as previously described (Fang et al., 2006). For western blot analyses, anti-CtBP (1:1000), anti-Pc (1:1000), anti-UTX (1:1000), anti-CBP (1:1000), αSer2-P (1:2000), anti-Fs(1)h (1:1000) and anti-tubulin (1:10,000) were used. Co-IP assay was performed according to standard procedures with anti-CtBP (10 µl), anti-CBP (10 µl), anti-UTX (10 µl), anti-Fs(1)h (10 µl) or normal IgG (5 µg). An initial protein-protein crosslinking step, incubating cells in a 5 mM dimethyl 3,30-dithio-bis(propionimidate) dihydrochloride (DTBP, Sigma-Aldrich) solution for 30-60 min on ice, was included in the co-IP experiments between CtBP and UTX, CBP, as well as Fs(1)h. ChIP assays were performed essentially as previously described (Fang et al., 2006). Approximately three million cells and anti-CtBP (10 µl), anti-Pc (2 µl), anti-CBP (2 µl), anti-UTX (2 µl), anti-H3K27me3 (2 µl), anti-H3K27ac (2 µl), anti-RNA Pol II (αCTD, 2 µl), anti- RNA Pol II Ser2-P (αSer2-P, 2 µl) antibodies or normal IgG (5 µg) were used per ChIP assay. All primers for dsRNA synthesis and PCR are listed in Table S1.

### RNA extractions and RT real-time quantitative PCR

Total RNA was extracted from cells or wing imaginal discs (~20 discs and ~1 µg total RNA yielding) using Trizol total RNA isolation reagent (Invitrogen). cDNA was synthesized with oligo-$(dT)_{18}$ using the Superscript III First Strand Synthesis System (Invitrogen) according to the manufacturer's instructions. qPCR amplification was then performed on iCycler iQ™ Real time PCR Detection System (Bio-Rad) with FastStart Universal SYBR green Master Mix (Roche Applied Science). The Ct values were determined by the absolute quantification method using standard curves. For all RT real-time quantitative PCR (RT-qPCR) experiments, the expression of genes was normalized to *β-Tubulin at 56D*. At least three independent experiments were performed for each assay. RT-qPCR primers for the respective genes are listed in Table S1.

### RNA-seq and bioinformatics

Total RNA was extracted from RNAi-treated Kc cells using Trizol total RNA isolation reagent (Invitrogen). RNA-seq data were obtained by the service provided by BGI from their deep sequencing platform build on the Illumina HiSeqTM 2000. RNA-seq data have been deposited in Gene Expression Omnibus under accession number GSE88807. The clean reads were then subject to further analysis based on the RNA-seq pipeline, using the open source Bowtie, TopHat, CuffLinks and CummeRbund software suite, built in our lab (Trapnell et al., 2012). Briefly, reads were mapped to the *Drosophila melanogaster* genome (BDGP5.25, the fruit fly iGenome

package, Ensemble build) using Bowtie (v2.2.4) (Langmead and Salzberg, 2012) and the splice junctions were determined from the mapped reads using TopHat (v2.0.13) (Kim et al., 2013). Cufflink (v 2.2.1) (Trapnell et al., 2012) was used for calculating expression levels in fragments per kilobase of exon per million fragments mapped (FPKM), data visualization and measuring expression levels. The Cuffdiff program within Cufflinks was used to test for statistically significant differences in transcript expression between different RNAi-treated cells. We restricted our analysis to 11,282 protein-coding genes across all nine samples. The downstream statistical analyses and plots were performed in R (v3.1.1; http://www.r-project.org/). We then selected 381 PcG target genes for further analysis, using the rule that expressional fold increase $\geq 2$ and $P \leq 0.05$ (unpaired two-tailed Student's *t*-test) (Fig. S3; Table S2).

For bioinformatics analyses, heatmaps and cluster analyses were generated in R with the function pheatmap of the g plots package (Liquet et al., 2012). Supervised hierarchical clustering was performed according to Euclidean distance using Ward's Method (Murtagh and Legendre, 2011). GO analysis was conducted using DAVID (Huang et al., 2009), Cytoscape (v3.4.0) and a BiNGO plugin (v3.0.3) (Maere et al., 2005; Saito et al., 2012) with chosen lists of genes based on the clustering describe above. We used the hyper-geometric test and the Benjamini–Hochberg FDR correction method (Benjamini Y, 1995), and a 0.001 significance level due to the high proportion of associated GO terms.

## Statistical analysis

For statistical analysis, experiments were performed at least three times. Data was presented as the mean± s.e.m. Statistical analyses, except those in bioinformatics, were performed using GraphPad Prism in which proper statistical methods and the $\alpha$ value were applied and indicated in each figure. The statistical analysis for ChIP-qPCR in Figs 5 and 6 was performed using one-way ANOVA followed by Tukey's multiple comparison tests (Table S4).

### Acknowledgements

The authors thank Drs Ken Cadigan, Xiang-Dong Liu and Yu-Feng Pan for critical reading of the paper. We also thank Dr Ken Cadigan and the Bloomington *Drosophila* Stock Center, the Vienna *Drosophila* RNAi Center and the Developmental Studies Hybridoma Bank for flies, cell lines and antibodies.

### Competing interests

The authors declare no competing or financial interests.

### Author contributions

Conceptualization: M.F.; Methodology: Q.C., L.-Y.Y., Q.W., L.Y.; Software: Q.C., Q.W., J.L.; Validation: L.Y.; Formal analysis: C.-L.B., H.X.; Investigation: C.-L.B., L.-Y.Y., H.-Y.W., L.C.; Resources: Q.C., P.W., J.L., F.T.; Data curation: C.-L.B., L.-Y.Y., P.W., R.W., F.T.; Writing - original draft: C.-L.B.; Visualization: R.W.; Supervision: H.X., M.F.; Project administration: C.-L.B., M.F.; Funding acquisition: M.F.

### Funding

This work was supported by grants from the National Natural Science Foundation of China [31271321 and 31471376 to M.F., 31301146 to H.X.]; and the Natural Science Foundation of Jiangsu Province [BK20141333 to M.F., BK20130605 to H.X.].

### Data availability

RNA-seq data have been deposited in GEO under accession number GSE88807.

### Peer review history

The peer review history is available online at https://journals.biologists.com/dev/article-lookup/doi/10.1242/dev.200153.

### References

**Basu, A. and Atchison, M. L.** (2010). CtBP levels control intergenic transcripts, PHO/YY1 DNA binding, and PcG recruitment to DNA. *J. Cell. Biochem.* **110**, 62-69. doi:10.1002/jcb.22487

**Beisel, C., Buness, A., Roustan-Espinosa, I. M., Koch, B., Schmitt, S., Haas, S. A., Hild, M., Katsuyama, T. and Paro, R.** (2007). Comparing active and repressed expression states of genes controlled by the Polycomb/Trithorax group proteins. *Proc. Natl. Acad. Sci. USA* **104**, 16615-16620. doi:10.1073/pnas.0701538104

**Benjamini Y, H. Y.** (1995). Controlling the false discovery rate: a practical and powerful approach to multiple testing. *J. R. Stat. Soc. B* **57**, 289-300. doi:10.1111/j.2517-6161.1995.tb02031.x

**Betschinger, J., Nichols, J., Dietmann, S., Corrin, P. D., Paddison, P. J. and Smith, A.** (2013). Exit from pluripotency is gated by intracellular redistribution of the bHLH transcription factor Tfe3. *Cell* **153**, 335-347. doi:10.1016/j.cell.2013.03.012

**Bhambhani, C., Chang, J. L., Akey, D. L. and Cadigan, K. M.** (2011). The oligomeric state of CtBP determines its role as a transcriptional co-activator and co-repressor of Wingless targets. *EMBO J.* **30**, 2031-2043. doi:10.1038/emboj.2011.100

**Bi, C., Meng, F., Yang, L., Cheng, L., Wang, P., Chen, M., Fang, M. and Xie, H.** (2018). CtBP represses Dpp signaling as a dimer. *Biochem. Biophys. Res. Commun.* **495**, 1980-1985. doi:10.1016/j.bbrc.2017.12.018

**Breen, T. R.** (1999). Mutant alleles of the Drosophila trithorax gene produce common and unusual homeotic and other developmental phenotypes. *Genetics* **152**, 319-344. doi:10.1093/genetics/152.1.319

**Castelli-Gair, J. E. and García-Bellido, A.** (1990). Interactions of Polycomb and trithorax with cis regulatory regions of Ultrabithorax during the development of Drosophila melanogaster. *EMBO J.* **9**, 4267-4275. doi:10.1002/j.1460-2075.1990.tb07875.x

**Chinnadurai, G.** (2002). CtBP, an unconventional transcriptional corepressor in development and oncogenesis. *Mol. Cell* **9**, 213-224. doi:10.1016/S1097-2765(02)00443-4

**Dcona, M. M., Morris, B. L., Ellis, K. C. and Grossman, S. R.** (2017). CtBP- an emerging oncogene and novel small molecule drug target: advances in the understanding of its oncogenic action and identification of therapeutic inhibitors. *Cancer Biol. Ther.* **18**, 379-391. doi:10.1080/15384047.2017.1323586

**Ding, B., Yuan, F., Damle, P. K., Litovchick, L., Drapkin, R. and Grossman, S. R.** (2020). CtBP determines ovarian cancer cell fate through repression of death receptors. *Cell Death Dis.* **11**, 286. doi:10.1038/s41419-020-2455-7

**Du, J., Zhang, J., He, T., Li, Y., Su, Y., Tie, F., Liu, M., Harte, P. J. and Zhu, A. J.** (2016). Stuxnet facilitates the degradation of polycomb protein during development. *Dev. Cell* **37**, 507-519. doi:10.1016/j.devcel.2016.05.013

**Duncan, I. M.** (1982). Polycomblike: a gene that appears to be required for the normal expression of the bithorax and antennapedia gene complexes of Drosophila melanogaster. *Genetics* **102**, 49-70. doi:10.1093/genetics/102.1.49

**Dupont, C. A., Dardalhon-Cuménal, D., Kyba, M., Brock, H. W., Randsholt, N. B. and Peronnet, F.** (2015). Drosophila Cyclin G and epigenetic maintenance of gene expression during development. *Epigenetics Chromatin* **8**, 18. doi:10.1186/s13072-015-0008-6

**Fang, M., Li, J., Blauwkamp, T., Bhambhani, C., Campbell, N. and Cadigan, K. M.** (2006). C-terminal-binding protein directly activates and represses Wnt transcriptional targets in Drosophila. *EMBO J.* **25**, 2735-2745. doi:10.1038/sj.emboj.7601153

**Fang, M., Ren, H., Liu, J., Cadigan, K. M., Patel, S. R. and Dressler, G. R.** (2009). Drosophila ptip is essential for anterior/posterior patterning in development and interacts with the PcG and trxG pathways. *Development* **136**, 1929-1938. doi:10.1242/dev.026559

**Gindhart, J. G., Jr and Kaufman, T. C.** (1995). Identification of Polycomb and trithorax group responsive elements in the regulatory region of the Drosophila homeotic gene Sex combs reduced. *Genetics* **139**, 797-814. doi:10.1093/genetics/139.2.797

**Gutiérrez, L., Zurita, M., Kennison, J. A. and Vázquez, M.** (2003). The Drosophila trithorax group gene tonalli (tna) interacts genetically with the Brahma remodeling complex and encodes an SP-RING finger protein. *Development* **130**, 343-354. doi:10.1242/dev.00222

**Hasson, P., Muller, B., Basler, K. and Paroush, Z.** (2001). Brinker requires two corepressors for maximal and versatile repression in Dpp signalling. *EMBO J.* **20**, 5725-5736. doi:10.1093/emboj/20.20.5725

**Hildebrand, J. D. and Soriano, P.** (2002). Overlapping and unique roles for C-terminal binding protein 1 (CtBP1) and CtBP2 during mouse development. *Mol. Cell. Biol.* **22**, 5296-5307. doi:10.1128/MCB.22.15.5296-5307.2002

**Huang, D. W., Sherman, B. T. and Lempicki, R. A.** (2009). Systematic and integrative analysis of large gene lists using DAVID bioinformatics resources. *Nat. Protoc.* **4**, 44-57. doi:10.1038/nprot.2008.211

**Ingham, P. W.** (1983). Differential expression of bithorax complex genes in the absence of the extra sex combs and trithorax genes. *Nature* **306**, 591-593. doi:10.1038/306591a0

**Kagey, M. H., Melhuish, T. A. and Wotton, D.** (2003). The polycomb protein Pc2 is a SUMO E3. *Cell* **113**, 127-137. doi:10.1016/S0092-8674(03)00159-4

**Kagey, M. H., Melhuish, T. A., Powers, S. E. and Wotton, D.** (2005). Multiple activities contribute to Pc2 E3 function. *EMBO J.* **24**, 108-119. doi:10.1038/sj.emboj.7600506

**Karch, F., Weiffenbach, B., Peifer, M., Bender, W., Duncan, I., Celniker, S., Crosby, M. and Lewis, E. B.** (1985). The abdominal region of the bithorax complex. *Cell* **43**, 81-96. doi:10.1016/0092-8674(85)90014-5

**Kennison, J. A. and Tamkun, J. W.** (1988). Dosage-dependent modifiers of polycomb and antennapedia mutations in Drosophila. *Proc. Natl. Acad. Sci. USA* **85**, 8136-8140. doi:10.1073/pnas.85.21.8136

**Kim, J. H., Cho, E. J., Kim, S. T. and Youn, H. D.** (2005). CtBP represses p300-mediated transcriptional activation by direct association with its bromodomain. *Nat. Struct. Mol. Biol.* **12**, 423-428. doi:10.1038/nsmb924

**Kim, D., Pertea, G., Trapnell, C., Pimentel, H., Kelley, R. and Salzberg, S. L.** (2013). TopHat2: accurate alignment of transcriptomes in the presence of insertions, deletions and gene fusions. *Genome Biol.* **14**, R36. doi:10.1186/gb-2013-14-4-r36

**Kim, T. W., Kang, B.-H., Jang, H., Kwak, S., Shin, J., Kim, H., Lee, S.-E., Lee, S.-M., Lee, J.-H., Kim, J.-H. et al.** (2015). Ctbp2 modulates NuRD-mediated deacetylation of H3K27 and facilitates PRC2-mediated H3K27me3 in active embryonic stem cell genes during exit from pluripotency. *Stem Cells* **33**, 2442-2455. doi:10.1002/stem.2046

**Komarnitsky, P., Cho, E. J. and Buratowski, S.** (2000). Different phosphorylated forms of RNA polymerase II and associated mRNA processing factors during transcription. *Genes Dev.* **14**, 2452-2460. doi:10.1101/gad.824700

**Langmead, B. and Salzberg, S. L.** (2012). Fast gapped-read alignment with Bowtie 2. *Nat. Methods* **9**, 357-359. doi:10.1038/nmeth.1923

**Lewis, E. B.** (1978). A gene complex controlling segmentation in Drosophila. *Nature* **276**, 565-570. doi:10.1038/276565a0

**Liquet, B., Le Cao, K. A., Hocini, H. and Thiébaut, R.** (2012). A novel approach for biomarker selection and the integration of repeated measures experiments from two assays. *BMC Bioinformatics* **13**, 325. doi:10.1186/1471-2105-13-325

**Maere, S., Heymans, K. and Kuiper, M.** (2005). BiNGO: a Cytoscape plugin to assess overrepresentation of gene ontology categories in biological networks. *Bioinformatics* **21**, 3448-3449. doi:10.1093/bioinformatics/bti551

**Müller, J. and Bienz, M.** (1991). Long range repression conferring boundaries of Ultrabithorax expression in the Drosophila embryo. *EMBO J.* **10**, 3147-3155. doi:10.1002/j.1460-2075.1991.tb04876.x

**Murtagh, F. and Legendre, P.** (2011). Ward's hierarchical clustering method: clustering criterion and agglomerative algorithm. *arXiv*. doi:10.48550/arXiv.1111.6285

**Nibu, Y., Zhang, H., Bajor, E., Barolo, S., Small, S. and Levine, M.** (1998a). dCtBP mediates transcriptional repression by Knirps, Kruppel and Snail in the Drosophila embryo. *EMBO J.* **17**, 7009-7020. doi:10.1093/emboj/17.23.7009

**Nibu, Y., Zhang, H. and Levine, M.** (1998b). Interaction of short-range repressors with Drosophila CtBP in the embryo. *Science* **280**, 101-104. doi:10.1126/science.280.5360.101

**Orlando, V., Jane, E. P., Chinwalla, V., Harte, P. J. and Paro, R.** (1998). Binding of trithorax and Polycomb proteins to the bithorax complex: dynamic changes during early Drosophila embryogenesis. *EMBO J.* **17**, 5141-5150. doi:10.1093/emboj/17.17.5141

**Panganiban, G., Sebring, A., Nagy, L. and Carroll, S.** (1995). The development of crustacean limbs and the evolution of arthropods. *Science* **270**, 1363-1366. doi:10.1126/science.270.5240.1363

**Papp, B. and Müller, J.** (2006). Histone trimethylation and the maintenance of transcriptional ON and OFF states by trxG and PcG proteins. *Genes Dev.* **20**, 2041-2054. doi:10.1101/gad.388706

**Parks, A. L., Cook, K. R., Belvin, M., Dompe, N. A., Fawcett, R., Huppert, K., Tan, L. R., Winter, C. G., Bogart, K. P., Deal, J. E. et al.** (2004). Systematic generation of high-resolution deletion coverage of the Drosophila melanogaster genome. *Nat. Genet.* **36**, 288-292. doi:10.1038/ng1312

**Pattatucci, A. M. and Kaufman, T. C.** (1991). The homeotic gene Sex combs reduced of Drosophila melanogaster is differentially regulated in the embryonic and imaginal stages of development. *Genetics* **129**, 443-461. doi:10.1093/genetics/129.2.443

**Phippen, T. M., Sweigart, A. L., Moniwa, M., Krumm, A., Davie, J. R. and Parkhurst, S. M.** (2000). Drosophila C-terminal binding protein functions as a context-dependent transcriptional co-factor and interferes with both mad and groucho transcriptional repression. *J. Biol. Chem.* **275**, 37628-37637. doi:10.1074/jbc.M004234200

**Piunti, A. and Shilatifard, A.** (2016). Epigenetic balance of gene expression by Polycomb and COMPASS families. *Science* **352**, aad9780. doi:10.1126/science.aad9780

**Poortinga, G., Watanabe, M. and Parkhurst, S. M.** (1998). Drosophila CtBP: a Hairy-interacting protein required for embryonic segmentation and hairy-mediated transcriptional repression. *EMBO J.* **17**, 2067-2078. doi:10.1093/emboj/17.7.2067

**Postigo, A. A. and Dean, D. C.** (1999). ZEB represses transcription through interaction with the corepressor CtBP. *Proc. Natl. Acad. Sci. USA* **96**, 6683-6688. doi:10.1073/pnas.96.12.6683

**Ray, S. K., Li, H. J., Metzger, E., Schüle, R. and Leiter, A. B.** (2014). CtBP and associated LSD1 are required for transcriptional activation by NeuroD1 in gastrointestinal endocrine cells. *Mol. Cell. Biol.* **34**, 2308-2317. doi:10.1128/MCB.01600-13

**Saito, R., Smoot, M. E., Ono, K., Ruscheinski, J., Wang, P.-L., Lotia, S., Pico, A. R., Bader, G. D. and Ideker, T.** (2012). A travel guide to Cytoscape plugins. *Nat. Methods* **9**, 1069-1076. doi:10.1038/nmeth.2212

**Samkurashvili, I. and Luse, D. S.** (1998). Structural changes in the RNA polymerase II transcription complex during transition from initiation to elongation. *Mol. Cell. Biol.* **18**, 5343-5354. doi:10.1128/MCB.18.9.5343

**Schaeper, U., Boyd, J. M., Verma, S., Uhlmann, E., Subramanian, T. and Chinnadurai, G.** (1995). Molecular cloning and characterization of a cellular phosphoprotein that interacts with a conserved C-terminal domain of adenovirus E1A involved in negative modulation of oncogenic transformation. *Proc. Natl. Acad. Sci. USA* **92**, 10467-10471. doi:10.1073/pnas.92.23.10467

**Schwartz, Y. B., Kahn, T. G., Nix, D. A., Li, X.-Y., Bourgon, R., Biggin, M. and Pirrotta, V.** (2006). Genome-wide analysis of Polycomb targets in Drosophila melanogaster. *Nat. Genet.* **38**, 700-705. doi:10.1038/ng1817

**Sewalt, R. G., Gunster, M. J., van der Vlag, J., Satijn, D. P. and Otte, A. P.** (1999). C-Terminal binding protein is a transcriptional repressor that interacts with a specific class of vertebrate Polycomb proteins. *Mol. Cell. Biol.* **19**, 777-787. doi:10.1128/MCB.19.1.777

**Shearn, A.** (1989). The ash-1, ash-2 and trithorax genes of Drosophila melanogaster are functionally related. *Genetics* **121**, 517-525. doi:10.1093/genetics/121.3.517

**Shi, Y., Sawada, J., Sui, G., Affar el, B., Whetstine, J. R., Lan, F., Ogawa, H., Luke, M. P.-S. and Nakatani, Y.** (2003). Coordinated histone modifications mediated by a CtBP co-repressor complex. *Nature* **422**, 735-738. doi:10.1038/nature01550

**Simon, J., Chiang, A., Bender, W., Shimell, M. J. and O'Connor, M.** (1993). Elements of the Drosophila bithorax complex that mediate repression by Polycomb group products. *Dev. Biol.* **158**, 131-144. doi:10.1006/dbio.1993.1174

**Singh, N. P. and Mishra, R. K.** (2014). Role of abd-A and Abd-B in development of abdominal epithelia breaks posterior prevalence rule. *PLoS Genet.* **10**, e1004717. doi:10.1371/journal.pgen.1004717

**Srinivasan, L. and Atchison, M. L.** (2004). YY1 DNA binding and PcG recruitment requires CtBP. *Genes Dev.* **18**, 2596-2601. doi:10.1101/gad.1228204

**Stankiewicz, T. R., Gray, J. J., Winter, A. N. and Linseman, D. A.** (2014). C-terminal binding proteins: central players in development and disease. *Biomol. Concepts* **5**, 489-511. doi:10.1515/bmc-2014-0027

**Steffen, P. A. and Ringrose, L.** (2014). What are memories made of? How Polycomb and Trithorax proteins mediate epigenetic memory. *Nat. Rev. Mol. Cell Bio.* **15**, 340-356. doi:10.1038/nrm3789

**Subramanian, T. and Chinnadurai, G.** (2003). Association of class I histone deacetylases with transcriptional corepressor CtBP. *FEBS Lett.* **540**, 255-258. doi:10.1016/S0014-5793(03)00275-8

**Tarleton, H. P. and Lemischka, I. R.** (2010). Delayed differentiation in embryonic stem cells and mesodermal progenitors in the absence of CtBP2. *Mech. Dev.* **127**, 107-119. doi:10.1016/j.mod.2009.10.002

**Tie, F., Banerjee, R., Stratton, C. A., Prasad-Sinha, J., Stepanik, V., Zlobin, A., Diaz, M. O., Scacheri, P. C. and Harte, P. J.** (2009). CBP-mediated acetylation of histone H3 lysine 27 antagonizes Drosophila Polycomb silencing. *Development* **136**, 3131-3141. doi:10.1242/dev.037127

**Tie, F., Banerjee, R., Fu, C., Stratton, C. A., Fang, M. and Harte, P. J.** (2016). Polycomb inhibits histone acetylation by CBP by binding directly to its catalytic domain. *Proc. Natl. Acad. Sci. USA* **113**, E744-E753. doi:10.1073/pnas.1515465113

**Trapnell, C., Roberts, A., Goff, L., Pertea, G., Kim, D., Kelley, D. R., Pimentel, H., Salzberg, S. L., Rinn, J. L. and Pachter, L.** (2012). Differential gene and transcript expression analysis of RNA-seq experiments with TopHat and Cufflinks. *Nat. Protoc.* **7**, 562-578. doi:10.1038/nprot.2012.016

**White, R. A. and Wilcox, M.** (1984). Protein products of the bithorax complex in Drosophila. *Cell* **39**, 163-171. doi:10.1016/0092-8674(84)90202-2

**Wirén, M., Silverstein, R. A., Sinha, I., Walfridsson, J., Lee, H. M., Laurenson, P., Pillus, L., Robyr, D., Grunstein, M. and Ekwall, K.** (2005). Genomewide analysis of nucleosome density histone acetylation and HDAC function in fission yeast. *EMBO J.* **24**, 2906-2918. doi:10.1038/sj.emboj.7600758

**Wu, C., Ding, X., Li, Z., Huang, Y., Xu, Q., Zou, R., Zhao, M., Chang, H., Jiang, C., La, X. et al.** (2021). CtBP modulates Snail-mediated tumor invasion in Drosophila. *Cell Death Discov.* **7**, 202. doi:10.1038/s41420-021-00516-x

**Yang, L., Meng, F., Ma, D., Xie, W. and Fang, M.** (2013). Bridging decapentaplegic and wingless signaling in Drosophila wings through repression of naked cuticle by Brinker. *Development* **140**, 413-422. doi:10.1242/dev.082578

**Zhang, C., Hong, Z., Ma, W., Ma, D., Qian, Y., Xie, W., Tie, F. and Fang, M.** (2013). Drosophila UTX coordinates with p53 to regulate ku80 expression in response to DNA damage. *PLoS One* **8**, e78652. doi:10.1371/journal.pone.0078652

**Zink, D. and Paro, R.** (1995). Drosophila Polycomb-group regulated chromatin inhibits the accessibility of a trans-activator to its target DNA. *EMBO J.* **14**, 5660-5671. doi:10.1002/j.1460-2075.1995.tb00253.x

## Figure S1

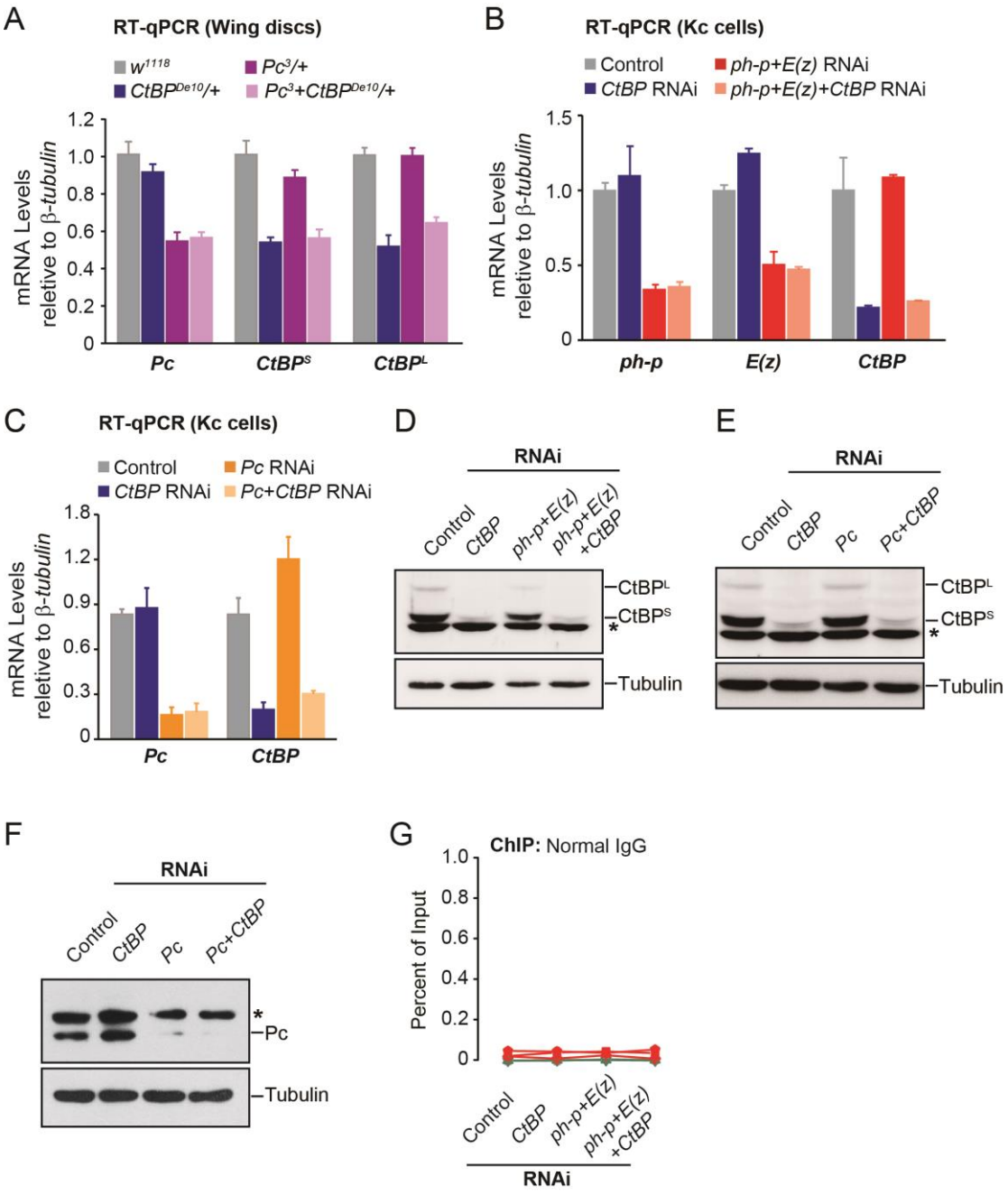


**Fig. S1. IgG ChIP controls and the verification of RNAi efficiency in wing discs and Kc cells.**

**(A)** RT-qPCR analysis of mRNA levels of *Pc* (A) and two *CtBP* transcripts [short ($CtBP^S$) and long ($CtBP^L$) forms] in the wing imaginal discs with genotypes indicated. **(B-C)** RT-qPCR analyses of mRNA levels (relative to β-*tubulin*) of genes in Kc cells with different combinations of RNAi treatments targeting *ph-p*, *E(z)*, *Pc* and *CtBP* and of control dsRNA, as indicated. **(D-F)** Verification of the protein levels of Pc and CtBP (CtBPS and CtBPL) in Kc cells subjected to different RNAi treatments as indicated. * indicated the nonspecific signals. Note that all genes were efficiently knocked down within comparable levels upon the different RNAi treatments. **(G)** ChIP-qPCR signals of normal IgG were measured and expressed as in Figure 5-6.

## Figure S2

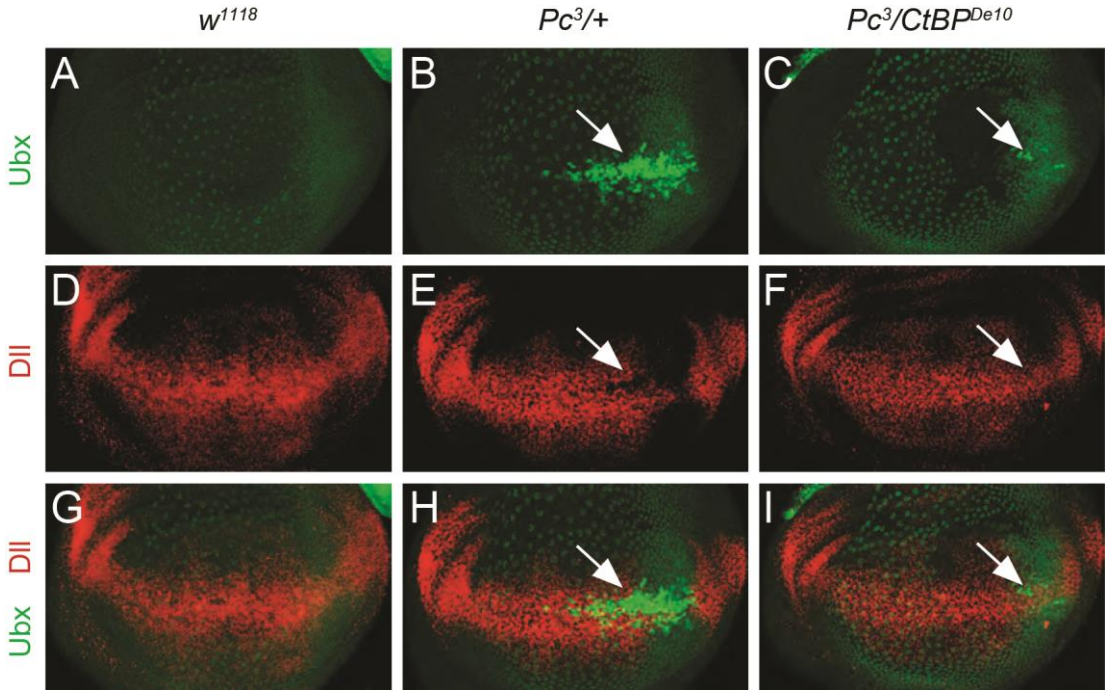


**Fig. S2. CtBP is required for Ubx to repress Dll expresion in wing imaginal disc.**

**(A-I)** Representative confocal images of the late 3rd instar wing imaginal discs, with genotypes annotated above, stained for Ubx (A-C) and Distal-less (Dll, D-F). (G-I) are merged from (A-F). Note the complementation of ectopic Ubx and the reduced Dll signals (arrows).

## Figure S3

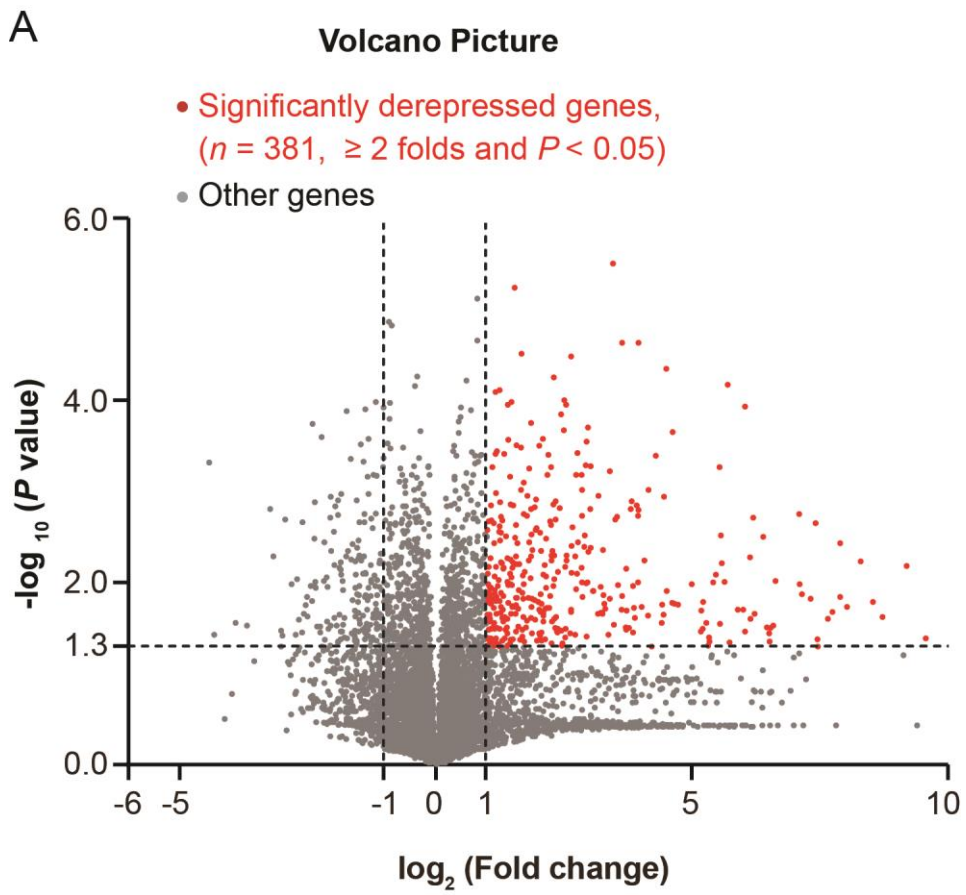


**Fig. S3. The selection of PcG repressed genes in Kc cells.**

**(A)** Volcano Plots of differentially expressed genes (DEG) between cells treated with control and *ph-p+E(z)* RNAi, as determined by the RNA-seq analysis pipeline (see Materials and Methods for detail). Of 11,282 genes with sound seq data, 381 were selected as PcG repressed genes (dots in red), based on the rule as indicated. The dashed lines indicate $P = 0.05$, $\log_2$[Fold change] = -1 and 1, respectively.

## Figure S4

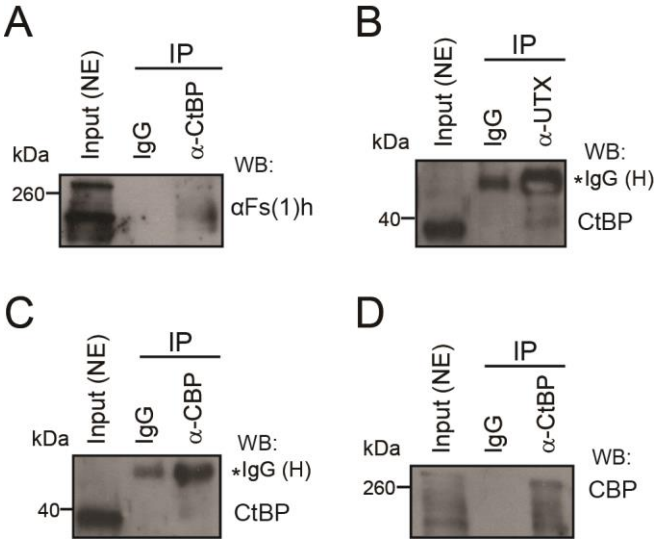


**Fig. S4. CtBP interacts with UTX, CBP and Fs(1)h.**

Western blots by antibodies indicated (to the right) of nuclear extracts (NE, 10% input), co-immunoprecipitates (IP) of normal IgG (IgG) and the indicated antibodies in Kc cells.

**Table S1.** List of primer sequences for dsRNA templates, RT-qPCR and ChIP analysis.

| | | |
|---|---|---|
| dsRNA | Control | GAATTAATACGACTCACTATAGGGAGAAT GATTGAACAAGATGGATTGCACGCA; GAATTAATACGACTCACTATAGGGAGAAAT ATCACGGGTAGCCAACGCTATGTCCT. |
| | *CtBP* | GAATTAATACGACTCACTATAGGGAGAAT GCACAAAGCACCTCCGAAATACACGA; GAATTAATACGACTCACTATAGGGAGAGC ACCAGGTCGCATCTGTTTAATTGTGAAT. |
| | *Pc* | GAATTAATACGACTCACTATAGGGAGAGCG TTAAGAAGGGCGTCGTGGAGTACC; GAATTAATACGACTCACTATAGGGAGAGGA GTTACCTGCTGGGTCGGCTGAGG. |
| | *ph-p* | GAATTAATACGACTCACTATAGGGAGAGGT CACAATTACCAACCAGAGCAGCACTCC; GAATTAATACGACTCACTATAGGGAGACGT GGTTGAAGTTGATGTTGCGGACG. |
| | *E(z)* | GAATTAATACGACTCACTATAGGGAGACGA GTCGAAGGTTTGGCAGGCTAAA; GAATTAATACGACTCACTATAGGGAGATTCT TCCACATCGGGCTTAACATCC. |
| RT-qPCR | β-*tubulin56D* | AGACCTACTGCATCGACAAC; GACAAGATGGTTCAGGTCAC. |
| | *CtBP* | ACCTTACAATGGCGCACTGAA; TGCGGTGTGCAAATCAGATT. |
| | *CtBP*$^{S}$ | AACGAACCTTACAATGGCGC; GGTGTGCAAATCAGATTTGGG. |
| | *CtBP*$^{L}$ | CGCTTGGAATTGTGAGTAGCC; TCACCTCCGTTTTTATGCTCG. |
| | *Pc* | GTTCCAGCCCTTCCACTTGAC; ATCATCCAAAAGCGCGTTAAG. |
| | *ph-p* | AGCAACAGGCGACGAATCTC; TTCTGCAGGGTGATCGGAGT. |
| | *E(z)* | GCCATCAGCGCTAACTTTCC; TGGTGCTCCGTAAGCTCAATG. |
| | *Antp* | ATGGACCTCTGTCACGTCGG; CAGGCGCAGTTGGGCTATAC. |
| | *Ubx* | AGAATCTCTTGCGGGCTCAC; GCAGACCATTTGTACCTAGCCA. |
| | *abd-A* | GTCGTTTGTGGCGATTTCAAC; AAGCGAGTGTAGGTCTGGCG. |
| | *Abd-B* | CAGCGAGAACTACTCCAGCTCAG; CACTGCTCCCACGGATAATC. |
| ChIP | Antp P1 | TGGCGCGCTTCGATATAAAC; CCAAACATCCACTTGCCGAC. |
| | Antp P2 | GCAGTCGGATGATTAATGGCA; CATCCCCATCTCCATTGCAG. |
| | bxd PRE | TAGTCTTATCTGTATCTCGCTCTTA; CAGAACCAAAGTGCCGATAACTC. |
| | bx PRE | CCATAAGAAATGCCACTTTGC; CTCTCACTCTCTCACTGTGAT. |
| | Ubx Pro | TCCAATCCGTTGCCATCGAACGAA; TTAGGCCGAGTCGAGTGAGTTGAG. |
| | Ubx Int | CCGAACATGAGAGATGGAAAA; AAAGTGCCGACAATGCAGTTA. |

**Table S2.** List of 381 PcG repressed genes as in Figure 3A.

| *CtBP* co-activated genes | | *CtBP* unaffected genes | | *CtBP* co-repressed genes | |
|---|---|---|---|---|---|
| **Flybase ID** | **Gene name (short)** | **Flybase ID** | **Gene name (short)** | **Flybase ID** | **Gene name (short)** |
| FBgn0000014 | *abd-A* | FBgn0000037 | *mAcR-60C* | FBgn0000071 | *Ama* |
| FBgn0000015 | *Abd-B* | FBgn0000043 | *Act42A* | FBgn0000099 | *ap* |
| FBgn0000157 | *Dll* | FBgn0000233 | *btd* | FBgn0000439 | *Dfd* |
| FBgn0000179 | *bi* | FBgn0000250 | *cact* | FBgn0000576 | *ems* |
| FBgn0000251 | *cad* | FBgn0000256 | *capu* | FBgn0000636 | *Fas3* |
| FBgn0000363 | *cpo* | FBgn0000320 | *eya* | FBgn0001235 | *hth* |
| FBgn0000459 | *disco* | FBgn0000337 | *cn* | FBgn0003053 | *peb* |
| FBgn0000490 | *dpp* | FBgn0000411 | *D* | FBgn0003159 | *ptr* |
| FBgn0000659 | *fkh* | FBgn0000448 | *Hr46* | FBgn0003997 | *W* |
| FBgn0001114 | *Glt* | FBgn0000489 | *Pka-C3* | FBgn0004858 | *elB* |
| FBgn0001138 | *grn* | FBgn0001319 | *kn* | FBgn0011706 | *rpr* |
| FBgn0001147 | *gsb-n* | FBgn0001325 | *Kr* | FBgn0013771 | *Cyp6a9* |
| FBgn0002522 | *lab* | FBgn0001967 | *nimC3* | FBgn0013995 | *Calx* |
| FBgn0003067 | *Pepck* | FBgn0002576 | *lz* | FBgn0014019 | *Rh5* |
| FBgn0003423 | *slgA* | FBgn0002917 | *na* | FBgn0015575 | *alpha-Est7* |
| FBgn0003460 | *so* | FBgn0002931 | *net* | FBgn0015766 | *Msr-110* |
| FBgn0003495 | *spz* | FBgn0002945 | *nkd* | FBgn0016675 | *Lectin-galC1* |
| FBgn0003513 | *ss* | FBgn0002973 | *numb* | FBgn0019643 | *Dat* |
| FBgn0003651 | *svp* | FBgn0003002 | *opa* | FBgn0020415 | *Idgf2* |
| FBgn0003717 | *Tl* | FBgn0003117 | *pnr* | FBgn0020762 | *Atet* |
| FBgn0003866 | *tsh* | FBgn0003254 | *rib* | FBgn0024290 | *Slob* |
| FBgn0003944 | *Ubx* | FBgn0003435 | *sm* | FBgn0026315 | *Ugt35a* |
| FBgn0003975 | *vg* | FBgn0003463 | *sog* | FBgn0026415 | *Idgf4* |
| FBgn0004102 | *oc* | FBgn0003749 | *trh* | FBgn0027070 | *CG17322* |
| FBgn0004360 | *Wnt2* | FBgn0003969 | *vap* | FBgn0027356 | *Amph* |
| FBgn0004394 | *pdm2* | FBgn0004009 | *wg* | FBgn0027556 | *CG4928* |
| FBgn0004435 | *Galpha49B* | FBgn0004575 | *Syn* | FBgn0030156 | *CG15247* |
| FBgn0004567 | *slp2* | FBgn0005624 | *Psc* | FBgn0030160 | *CG9691* |
| FBgn0004579 | *salm* | FBgn0008646 | *E5* | FBgn0031362 | *CG17646* |
| FBgn0004595 | *pros* | FBgn0008654 | *Su(z)2* | FBgn0031791 | *CG9486* |
| FBgn0004607 | *zfh2* | FBgn0010225 | *Gel* | FBgn0032318 | *CG14072* |
| FBgn0004629 | *Cys* | FBgn0010313 | *corto* | FBgn0032422 | *CG6579* |
| FBgn0004795 | *retn* | FBgn0010381 | *Drs* | FBgn0032843 | *CG10730* |
| FBgn0005677 | *dac* | FBgn0010453 | *Wnt4* | FBgn0032886 | *CG9328* |
| FBgn0011722 | *Tig* | FBgn0010768 | *sqz* | FBgn0032897 | *CG9336* |
| FBgn0013763 | *Chit* | FBgn0013469 | *klu* | FBgn0032899 | *CG9338* |
| FBgn0013772 | *Cyp6a8* | FBgn0015872 | *Drip* | FBgn0033408 | *CG8800* |
| FBgn0013953 | *Esp* | FBgn0016059 | *Sema-1b* | FBgn0033504 | *CAP* |
| FBgn0014343 | *mirr* | FBgn0016660 | *H15* | FBgn0033981 | *Cyp6a21* |
| FBgn0015561 | *unpg* | FBgn0016930 | *smi35A* | FBgn0034198 | *CG11400* |
| FBgn0015576 | *alpha-Est8* | FBgn0020307 | *dve* | FBgn0034199 | *CG15917* |
| FBgn0015903 | *apt* | FBgn0020416 | *Idgf1* | FBgn0034200 | *CG11395* |
| FBgn0020445 | *E23* | FBgn0024150 | *Ac78C* | FBgn0034429 | *CG18607* |
| FBgn0020546 | *iab-4* | FBgn0024288 | *Sox100B* | FBgn0034733 | *CG4752* |
| FBgn0020912 | *Ptx1* | FBgn0024980 | *Syx4* | FBgn0035508 | *CG15005* |
| FBgn0023441 | *fus* | FBgn0025525 | *bab2* | FBgn0035975 | *PGRP-LA* |
| FBgn0024184 | *unc-4* | FBgn0025680 | *cry* | FBgn0036419 | *CG13482* |
| FBgn0024244 | *drm* | FBgn0026063 | *KP78b* | FBgn0036493 | *CG7255* |
| FBgn0025578 | *Lcp9* | FBgn0026189 | *prominin-like* | FBgn0036782 | *CG7320* |

**Table S2.** Continued.

| *CtBP* co-activated genes | | *CtBP* unaffected genes | | *CtBP* co-repressed genes | |
|---|---|---|---|---|---|
| **Flybase ID** | **Gene name (short)** | **Flybase ID** | **Gene name (short)** | **Flybase ID** | **Gene name (short)** |
| FBgn0025693 | *CG11163* | FBgn0027348 | *bgm* | FBgn0037163 | *laza* |
| FBgn0026064 | *KP78a* | FBgn0027600 | *obst-B* | FBgn0037166 | *CG11426* |
| FBgn0026411 | *Lim1* | FBgn0028550 | *A3-3* | FBgn0037515 | *Sp7* |
| FBgn0027578 | *CG14526* | FBgn0028979 | *tio* | FBgn0038088 | *CG10126* |
| FBgn0027929 | *nimB1* | FBgn0029123 | *SoxN* | FBgn0038150 | *yellow-e3* |
| FBgn0028519 | *CG4500* | FBgn0029895 | *CG14441* | FBgn0038151 | *yellow-e2* |
| FBgn0028542 | *nimB4* | FBgn0030090 | *fend* | FBgn0038179 | *CG9312* |
| FBgn0028543 | *nimB2* | FBgn0030296 | *CG15196* | FBgn0038198 | *Npc2b* |
| FBgn0028936 | *nimB5* | FBgn0030340 | *CG15740* | FBgn0038261 | *CG14856* |
| FBgn0028940 | *Cyp28a5* | FBgn0030722 | *CG12395* | FBgn0038262 | *CG14857* |
| FBgn0029003 | *mab-21* | FBgn0030839 | *CG5613* | FBgn0038353 | *CG5399* |
| FBgn0029703 | *CG12692* | FBgn0031080 | *CG12655* | FBgn0038391 | *GATAe* |
| FBgn0029775 | *Vsx1* | FBgn0031081 | *Nep3* | FBgn0038720 | *CG6231* |
| FBgn0030452 | *CG4330* | FBgn0031170 | *CG1718* | FBgn0039075 | *CG4393* |
| FBgn0030723 | *dpr18* | FBgn0031397 | *CG15385* | FBgn0039905 | *CG2052* |
| FBgn0030796 | *CG4829* | FBgn0031910 | *CG15818* | FBgn0040730 | *CG15127* |
| FBgn0030816 | *CG16700* | FBgn0031920 | *CG6441* | FBgn0040732 | *CG16926* |
| FBgn0031327 | *CG5397* | FBgn0031927 | *CG13792* | FBgn0040827 | *CG13315* |
| FBgn0031389 | *CG4259* | FBgn0031970 | *CG7227* | FBgn0041711 | *yellow-e* |
| FBgn0031547 | *Sr-CIV* | FBgn0031993 | *CG8486* | FBgn0042696 | *Nfl* |
| FBgn0031646 | *CG2837* | FBgn0032120 | *CG33298* | FBgn0045064 | *bwa* |
| FBgn0031695 | *Cyp4ac3* | FBgn0032265 | *CG18301* | FBgn0050438 | *CG30438* |
| FBgn0031914 | *CG5973* | FBgn0032935 | *CG8678* | FBgn0050456 | *CG30456* |
| FBgn0031923 | *CG13791* | FBgn0033649 | *pyr* | FBgn0051116 | *CG31116* |
| FBgn0032086 | *CG17906* | FBgn0033756 | *CG17760* | FBgn0051287 | *CG31287* |
| FBgn0032124 | *CG17855* | FBgn0033787 | *CG13321* | FBgn0051313 | *CG31313* |
| FBgn0032493 | *CG15479* | FBgn0033791 | *Drl-2* | FBgn0051436 | *CG31436* |
| FBgn0032946 | *nrv3* | FBgn0034194 | *CG15611* | FBgn0051454 | *CG31454* |
| FBgn0032955 | *CG2201* | FBgn0034195 | *CG10956* | FBgn0053555 | *btsz* |
| FBgn0032978 | *CG15216* | FBgn0034196 | *CG15605* | FBgn0083919 | *Zasp52* |
| FBgn0033042 | *Tsp42A* | FBgn0034219 | *mthl4* | FBgn0085227 | *CG34198* |
| FBgn0033065 | *Cyp6w1* | FBgn0034389 | *Mctp* | FBgn0259175 | *ome* |
| FBgn0033250 | *CG14762* | FBgn0034417 | *CG15117* | FBgn0259244 | *CG42342* |
| FBgn0033387 | *CG8008* | FBgn0034428 | *CG18606* | FBgn0259736 | *CG42390* |
| FBgn0033483 | *egr* | FBgn0034476 | *Toll-7* | FBgn0260000 | *CG17570* |
| FBgn0033635 | *CG7777* | FBgn0034883 | *CG17664* | FBgn0260005 | *wtrw* |
| FBgn0033857 | *CG13335* | FBgn0035146 | *CG13893* | | |
| FBgn0033939 | *Oaz* | FBgn0035262 | *CG18171* | | |
| FBgn0034010 | *CG8157* | FBgn0035412 | *CG14957* | | |
| FBgn0034085 | *Ptp52F* | FBgn0035454 | *CG12029* | | |
| FBgn0034126 | *CG4398* | FBgn0035976 | *PGRP-LC* | | |
| FBgn0034140 | *CG8317* | FBgn0035977 | *PGRP-LF* | | |
| FBgn0034221 | *CG10764* | FBgn0036359 | *CG14105* | | |
| FBgn0034810 | *CG9895* | FBgn0036377 | *CG10710* | | |
| FBgn0034834 | *CG3162* | FBgn0036381 | *CG8745* | | |
| FBgn0034957 | *CG3121* | FBgn0036494 | *Toll-6* | | |
| FBgn0034985 | *CG3328* | FBgn0037005 | *CG5078* | | |
| FBgn0035282 | *CG13936* | FBgn0037060 | *CG10508* | | |
| FBgn0035453 | *CG10357* | FBgn0037698 | *CG16779* | | |
| FBgn0035583 | *CG13704* | FBgn0037989 | *CG14741* | | |
| FBgn0035623 | *mthl2* | FBgn0038243 | *CG8066* | | |

**Table S2.** Continued.

| *CtBP* co-activated genes | | *CtBP* unaffected genes | | *CtBP* co-repressed genes | |
|---|---|---|---|---|---|
| *Flybase ID* | *Gene name (short)* | *Flybase ID* | *Gene name (short)* | *Flybase ID* | *Gene name (short)* |
| FBgn0036620 | *CG4842* | FBgn0038416 | *CG17930* | | |
| FBgn0036904 | *trpml* | FBgn0039060 | *CG13836* | | |
| FBgn0036956 | *CG13813* | FBgn0039067 | *wda* | | |
| FBgn0037222 | *CG14642* | FBgn0039068 | *CG13827* | | |
| FBgn0037223 | *TwdlU* | FBgn0039648 | *CG14515* | | |
| FBgn0037228 | *CG1092* | FBgn0039818 | *CG11318* | | |
| FBgn0037487 | *CG14608* | FBgn0039927 | *CG11155* | | |
| FBgn0037937 | *Fer3* | FBgn0039938 | *Sox102F* | | |
| FBgn0037941 | *CG12594* | FBgn0040503 | *CG7763* | | |
| FBgn0038237 | *Pde6* | FBgn0041087 | *wun2* | | |
| FBgn0038832 | *CG15695* | FBgn0041229 | *Gr93a* | | |
| FBgn0039000 | *CG6954* | FBgn0043806 | *CG32032* | | |
| FBgn0039226 | *CG18410* | FBgn0046776 | *CG14033* | | |
| FBgn0039611 | *CG14528* | FBgn0050151 | *CG30151* | | |
| FBgn0039756 | *CG9743* | FBgn0051053 | *CG31053* | | |
| FBgn0040384 | *CG32795* | FBgn0051217 | *modSP* | | |
| FBgn0040502 | *CG8343* | FBgn0051778 | *CG31778* | | |
| FBgn0040813 | *Nplp2* | FBgn0051999 | *CG31999* | | |
| FBgn0041233 | *Gr59e* | FBgn0052121 | *CG32121* | | |
| FBgn0041234 | *Gr59f* | FBgn0052407 | *CG32407* | | |
| FBgn0041629 | *Hexo2* | FBgn0052712 | *CG32712* | | |
| FBgn0042105 | *CG18748* | FBgn0052987 | *CG32987* | | |
| FBgn0042650 | *disco-r* | FBgn0052988 | *CG32988* | | |
| FBgn0050043 | *CG30043* | FBgn0053173 | *CG33173* | | |
| FBgn0050054 | *CG30054* | FBgn0053533 | *lectin-37Db* | | |
| FBgn0050089 | *CG30089* | FBgn0053758 | *CG33758* | | |
| FBgn0050090 | *CG30090* | FBgn0053980 | *Vsx2* | | |
| FBgn0050461 | *CG30461* | FBgn0054003 | *nimB3* | | |
| FBgn0050463 | *CG30463* | FBgn0060296 | *pain* | | |
| FBgn0051038 | *CG31038* | FBgn0083973 | *CG34137* | | |
| FBgn0051051 | *CG31051* | FBgn0085218 | *CG34189* | | |
| FBgn0052843 | *Dh31-R1* | FBgn0085403 | *Rapgap1* | | |
| FBgn0053460 | *CG33460* | FBgn0085409 | *CG34380* | | |
| FBgn0053465 | *CG33465* | FBgn0086677 | *jeb* | | |
| FBgn0053532 | *lectin-37Da* | FBgn0250907 | *Cht3* | | |
| FBgn0053960 | *CG33960* | FBgn0259211 | *grh* | | |
| FBgn0053993 | *CG33993* | FBgn0259699 | *CG42353* | | |
| FBgn0054054 | *CG34054* | FBgn0260011 | *nimC4* | | |
| FBgn0065110 | *ppk10* | FBgn0260429 | *CG42524* | | |
| FBgn0085419 | *Rgk2* | FBgn0261059 | *Sfp78E* | | |
| FBgn0085424 | *nub* | FBgn0261260 | *CG42611* | | |
| FBgn0086680 | *vvl* | FBgn0261287 | *ymp* | | |
| FBgn0243514 | *eater* | FBgn0261545 | *CG42663* | | |
| FBgn0250821 | *CG14644* | | | | |
| FBgn0259192 | *CG42296* | | | | |
| FBgn0259240 | *Ten-a* | | | | |
| FBgn0259241 | *CG42339* | | | | |
| FBgn0259715 | *CG42369* | | | | |
| FBgn0259739 | *CG42393* | | | | |
| FBgn0259794 | *sinah* | | | | |
| FBgn0259896 | *nimC1* | | | | |
| FBgn0260642 | *Antp* | | | | |
| FBgn0261451 | *trol* | | | | |

**Table S3.** List of 73 PcG targets.

| *CtBP*-associated PcG targets | | *CtBP*-unassociated PcG targets | |
|---|---|---|---|
| ***Flybase ID*** | ***Gene name (short)*** | ***Flybase ID*** | ***Gene name (short)*** |
| FBgn0001147 | *gsb-n* | FBgn0000071 | *Ama* |
| FBgn0052988 | *CG32988* | FBgn0038391 | *GATAe* |
| FBgn0000490 | *dpp* | FBgn0000099 | *ap* |
| FBgn0003975 | *vg* | FBgn0000411 | *D* |
| FBgn0034810 | *CG9895* | FBgn0000576 | *ems* |
| FBgn0020912 | *Ptx1* | FBgn0003053 | *peb* |
| FBgn0004795 | *retn* | FBgn0000439 | *Dfd* |
| FBgn0001138 | *grn* | FBgn0001235 | *hth* |
| FBgn0003651 | *svp* | | |
| FBgn0029003 | *mab-21* | | |
| FBgn0004394 | *pdm2* | | |
| FBgn0000037 | *mAcR-60C* | | |
| FBgn0014343 | *mirr* | | |
| FBgn0023441 | *fus* | | |
| FBgn0003460 | *so* | | |
| FBgn0024184 | *unc-4* | | |
| FBgn0002522 | *lab* | | |
| FBgn0000014 | *abd-A* | | |
| FBgn0003513 | *ss* | | |
| FBgn0000015 | *Abd-B* | | |
| FBgn0029775 | *Vsx1* | | |
| FBgn0260642 | *Antp* | | |
| FBgn0015561 | *unpg* | | |
| FBgn0000179 | *bi* | | |
| FBgn0026411 | *Lim1* | | |
| FBgn0003944 | *Ubx* | | |
| FBgn0034883 | *CG17664* | | |
| FBgn0042650 | *disco-r* | | |
| FBgn0003254 | *rib* | | |
| FBgn0029123 | *SoxN* | | |
| FBgn0025525 | *bab2* | | |
| FBgn0033787 | *CG13321* | | |
| FBgn0008654 | *Su(z)2* | | |
| FBgn0002576 | *lz* | | |
| FBgn0016660 | *H15* | | |
| FBgn0001325 | *Kr* | | |
| FBgn0053980 | *Vsx2* | | |
| FBgn0005677 | *dac* | | |
| FBgn0004579 | *salm* | | |
| FBgn0004567 | *slp2* | | |
| FBgn0000157 | *Dll* | | |
| FBgn0004607 | *zfh2* | | |
| FBgn0000459 | *disco* | | |
| FBgn0004595 | *pros* | | |
| FBgn0033250 | *CG14762* | | |
| FBgn0001319 | *kn* | | |
| FBgn0003423 | *slgA* | | |
| FBgn0015903 | *apt* | | |
| FBgn0000659 | *fkh* | | |
| FBgn0003002 | *opa* | | |
| FBgn0000251 | *cad* | | |
| FBgn0003749 | *trh* | | |
| FBgn0013469 | *klu* | | |
| FBgn0026063 | *KP78b* | | |
| FBgn0026064 | *KP78a* | | |
| FBgn0004102 | *oc* | | |
| FBgn0052987 | *CG32987* | | |
| FBgn0086680 | *vvl* | | |
| FBgn0008646 | *E5* | | |
| FBgn0003117 | *pnr* | | |
| FBgn0004009 | *wg* | | |
| FBgn0024244 | *drm* | | |
| FBgn0259211 | *grh* | | |
| FBgn0005624 | *Psc* | | |
| FBgn0024288 | *Sox100B* | | |

Note: The genes are listed in the order of heatmaps in Figure 4B.

**Table S4.** List of *P* value as in Figure 5 B-G and Figure 6 A-B.

**Supplemental Table 4-1.** List of *P* value for data in Figure 5B

| | *P* value of ANOVA | Adjusted *P* value (post-hoc) | | | | | |
|---|---|---|---|---|---|---|---|
| | | *CtBP* RNAi VS. Control RNAi | *Ph+E(z)* RNAi VS. Control RNAi | *Ph+E(z)+CtBP* RNAi VS. Control RNAi | *Ph+E(z)* RNAi VS. *CtBP* RNAi | *Ph+E(z)+CtBP* RNAi VS. *CtBP* RNAi | *Ph+E(z)+CtBP* RNAi VS. *Ph+E(z)* RNAi |
| PRE (*Antp*) | 0.0027 | 0.0136 | 0.9199 | 0.0336 | 0.0061 | 0.9076 | 0.0143 |
| Promoter/ PRE (*Antp*) | 0.0007 | 0.0011 | 0.0251 | 0.0011 | 0.1161 | > 0.9999 | 0.1258 |
| PRE (*bx*) | 0.0404 | 0.0649 | 0.9528 | 0.1198 | 0.1342 | 0.9707 | 0.2423 |
| Promoter (*Ubx*) | 0.0034 | 0.0068 | 0.0131 | 0.0047 | 0.9542 | 0.9908 | 0.8522 |
| PRE (*bxd*) | 0.0793 | | | | | | |

**Supplemental Table 4-2.** List of *P* value for data in Figure 5C

| | *P* value of ANOVA | Adjusted *P* value (post-hoc) | | | | | |
|---|---|---|---|---|---|---|---|
| | | *CtBP* RNAi VS. Control RNAi | *Ph+E(z)* RNAi VS. Control RNAi | *Ph+E(z)+CtBP* RNAi VS. Control RNAi | *Ph+E(z)* RNAi VS. *CtBP* RNAi | *Ph+E(z)+CtBP* RNAi VS. *CtBP* RNAi | *Ph+E(z)+CtBP* RNAi VS. *Ph+E(z)* RNAi |
| PRE (*Antp*) | 0.0002 | 0.0041 | 0.0001 | 0.0014 | 0.0433 | 0.7985 | 0.1565 |
| Promoter/ PRE (*Antp*) | < 0.0001 | < 0.0001 | < 0.0001 | < 0.0001 | 0.0048 | 0.4000 | 0.0430 |
| PRE (*bx*) | < 0.0001 | 0.0045 | < 0.0001 | 0.0009 | 0.0009 | 0.5263 | 0.0044 |
| Promoter (*Ubx*) | 0.0628 | | | | | | |
| PRE (*bxd*) | 0.0034 | 0.7009 | 0.0029 | 0.2774 | 0.0112 | 0.8227 | 0.0362 |

**Supplemental Table 4-3.** List of *P* value for data in Figure 5D

| | *P* value of ANOVA | Adjusted *P* value (post-hoc) | | | | | |
|---|---|---|---|---|---|---|---|
| | | *CtBP* RNAi VS. Control RNAi | *Ph+E(z)* RNAi VS. Control RNAi | *Ph+E(z)+CtBP* RNAi VS. Control RNAi | *Ph+E(z)* RNAi VS. *CtBP* RNAi | *Ph+E(z)+CtBP* RNAi VS. *CtBP* RNAi | *Ph+E(z)+CtBP* RNAi VS. *Ph+E(z)* RNAi |
| PRE (*Antp*) | 0.0102 | 0.2414 | 0.0078 | 0.6453 | 0.1321 | 0.8192 | 0.0387 |
| Promoter/ PRE (*Antp*) | 0.0030 | 0.0809 | 0.0018 | 0.0547 | 0.0708 | 0.9919 | 0.1048 |
| PRE (*bx*) | 0.0201 | 0.2470 | 0.0127 | 0.2182 | 0.2163 | 0.9997 | 0.2448 |
| Promoter (*Ubx*) | 0.0039 | 0.0793 | 0.0026 | 0.2661 | 0.1142 | 0.8143 | 0.0330 |
| PRE (*bxd*) | 0.0128 | 0.7267 | 0.0350 | 0.8312 | 0.1530 | 0.3011 | 0.0111 |

**Supplemental Table 4-4.** List of *P* value for data in Figure 5E

| | *P* value of ANOVA | Adjusted *P* value (post-hoc) | | | | | |
|---|---|---|---|---|---|---|---|
| | | *CtBP* RNAi VS. Control RNAi | *Ph+E(z)* RNAi VS. Control RNAi | *Ph+E(z)+CtBP* RNAi VS. Control RNAi | *Ph+E(z)* RNAi VS. *CtBP* RNAi | *Ph+E(z)+CtBP* RNAi VS. *CtBP* RNAi | *Ph+E(z)+CtBP* RNAi VS. *Ph+E(z)* RNAi |
| PRE (*Antp*) | 0.0004 | 0.5788 | 0.0019 | > 0.9999 | 0.0005 | 0.5811 | 0.0019 |
| Promoter/ PRE (*Antp*) | 0.0008 | 0.9969 | 0.002 | 0.9943 | 0.0016 | > 0.9999 | 0.0015 |
| PRE (*bx*) | < 0.0001 | 0.1209 | < 0.0001 | 0.0448 | < 0.0001 | 0.8923 | < 0.0001 |
| Promoter (*Ubx*) | 0.0493 | 0.997 | 0.075 | > 0.9999 | 0.0991 | 0.9964 | 0.0736 |
| PRE (*bxd*) | 0.0017 | > 0.9999 | 0.0035 | 0.9998 | 0.0037 | > 0.9999 | 0.0039 |

**Table S4.** Continued.

**Supplemental Table 4-5.** List of *P* value for data in Figure 5F

| | *P* value of *ANOVA* | Adjusted *P* value (post-hoc) | | | | | |
|---|---|---|---|---|---|---|---|
| | | *CtBP* RNAi VS. Control RNAi | *Ph+E(z)* RNAi VS. Control RNAi | *Ph+E(z)+CtBP* RNAi VS. Control RNAi | *Ph+E(z)* RNAi VS. *CtBP* RNAi | *Ph+E(z)+CtBP* RNAi VS. *CtBP* RNAi | *Ph+E(z)+CtBP* RNAi VS. *Ph+E(z)* RNAi |
| PRE (*Antp*) | < 0.0001 | 0.0593 | 0.0008 | 0.0949 | < 0.0001 | 0.9864 | < 0.0001 |
| Promoter/ PRE (*Antp*) | 0.0015 | 0.8101 | 0.0072 | 0.8124 | 0.0025 | > 0.9999 | 0.0025 |
| PRE (*bx*) | 0.0598 | | | | | | |
| Promoter (*Ubx*) | 0.0335 | 0.9877 | 0.0746 | 0.9970 | 0.0474 | 0.9993 | 0.0563 |
| PRE (*bxd*) | 0.0051 | 0.9071 | 0.0419 | 0.3714 | 0.0168 | 0.7212 | 0.0043 |

**Supplemental Table 4-6.** List of *P* value for data in Figure 5G

| | *P* value of *ANOVA* | Adjusted *P* value (post-hoc) | | | | | |
|---|---|---|---|---|---|---|---|
| | | *CtBP* RNAi VS. Control RNAi | *Ph+E(z)* RNAi VS. Control RNAi | *Ph+E(z)+CtBP* RNAi VS. Control RNAi | *Ph+E(z)* RNAi VS. *CtBP* RNAi | *Ph+E(z)+CtBP* RNAi VS. *CtBP* RNAi | *Ph+E(z)+CtBP* RNAi VS. *Ph+E(z)* RNAi |
| PRE (*Antp*) | 0.0008 | 0.8396 | 0.0032 | 0.9403 | 0.0013 | 0.9929 | 0.0017 |
| Promoter/ PRE (*Antp*) | < 0.0001 | 0.2868 | 0.0005 | 0.7097 | < 0.0001 | 0.8277 | 0.0002 |
| PRE (*bx*) | 0.0082 | 0.9995 | 0.0143 | 0.1989 | 0.0123 | 0.1713 | 0.2996 |
| Promoter (*Ubx*) | 0.0177 | 0.9553 | 0.0875 | 0.6447 | 0.0428 | 0.8974 | 0.0166 |
| PRE (*bxd*) | < 0.0001 | > 0.9999 | < 0.0001 | 0.5810 | < 0.0001 | 0.5884 | < 0.0001 |

**Supplemental Table 4-7.** List of *P* value for data in Figure 6A

| | *P* value of *ANOVA* | Adjusted *P* value (post-hoc) | | | | | |
|---|---|---|---|---|---|---|---|
| | | *CtBP* RNAi VS. Control RNAi | *Ph+E(z)* RNAi VS. Control RNAi | *Ph+E(z)+CtBP* RNAi VS. Control RNAi | *Ph+E(z)* RNAi VS. *CtBP* RNAi | *Ph+E(z)+CtBP* RNAi VS. *CtBP* RNAi | *Ph+E(z)+CtBP* RNAi VS. *Ph+E(z)* RNAi |
| PRE (*Antp*) | 0.0026 | 0.3579 | 0.4256 | 0.0201 | 0.9993 | 0.0038 | 0.0046 |
| Promoter/ PRE (*Antp*) | 0.1409 | | | | | | |
| PRE (*bx*) | 0.2257 | | | | | | |
| Promoter (*Ubx*) | 0.0200 | 0.9996 | 0.0175 | 0.9807 | 0.0458 | 0.9948 | 0.0681 |
| PRE (*bxd*) | 0.0502 | | | | | | |

**Supplemental Table 4-8.** List of *P* value for data in Figure 6B

| | *P* value of *ANOVA* | Adjusted *P* value (post-hoc) | | | | | |
|---|---|---|---|---|---|---|---|
| | | *CtBP* RNAi VS. Control RNAi | *Ph+E(z)* RNAi VS. Control RNAi | *Ph+E(z)+CtBP* RNAi VS. Control RNAi | *Ph+E(z)* RNAi VS. *CtBP* RNAi | *Ph+E(z)+CtBP* RNAi VS. *CtBP* RNAi | *Ph+E(z)+CtBP* RNAi VS. *Ph+E(z)* RNAi |
| PRE (*Antp*) | 0.0063 | 0.7589 | 0.0110 | 0.7066 | 0.0064 | 0.3263 | 0.1239 |
| Promoter/ PRE (*Antp*) | 0.0012 | 0.7908 | 0.0022 | 0.2196 | 0.0017 | 0.0975 | 0.1203 |
| PRE (*bx*) | 0.7469 | | | | | | |
| Promoter (*Ubx*) | 0.7708 | | | | | | |
| PRE (*bxd*) | < 0.0001 | 0.9765 | < 0.0001 | 0.1845 | < 0.0001 | 0.4430 | < 0.0001 |

For each loci, data were analyzed by one-way *ANOVA*, followed by Tukey's multiple comparison tests.